

Shouvik Ghorui  
Jadavpur University, kolkata

### **Case Study 1**

CFD study of ventilation in a room maintained under negative-pressure to prevent airborne contamination

### **Case Study 2**

CFD study of deLaval nozzle with Fanno and Rayleigh condition

Mentored By  
Divyesh Variya & Prof. Janani srree Muralidharan

# CFD study of ventilation in a room maintained under negative-pressure to prevent airborne contamination

**Shouvik Ghorui**

Jadavpur University, Kolkata

## Abstract

Isolation rooms are used in hospitals for patients who suffer from diseases like tuberculosis, COVID-19, and severe acute respiratory syndrome. It is very crucial to protect doctors, nurses, and other health-care workers from patients with infectious diseases by the effective ventilation system. This case study studies different inlet-outlet configurations in order to determine the most suitable combination that will help prevent air-borne contamination in a negative pressure isolation room. Computational Fluid Dynamics is a technique that is used to analyse the indoor environment of a ventilated room and overall ventilation of air distribution systems. *blockMesh* utility is used for meshing a three-dimensional room of size  $4*4*2.5\text{ m}^3$ . Bed and patient are modelled in CAD software. The final finished mesh is done using *snappyHexMesh* utility of OpenFoam. Discretized conservation equations like continuity, momentum, energy and turbulence are solved simultaneously using CFD Open Source package **OpenFOAM® V-7.0** with *buoyantPimpleFoam* solver to simulate the flow Physics.

**Keywords:-** CFD, OpenFOAM, Negative pressure ventilation room, COVID-19

## 1. Introduction

Over the last few decades, the consciousness for air flow inside the room is increasing and its influence on the design of the air-conditioning and mechanical ventilation (ACMV) system is also an important factor. This is especially crucial in hospitals where air-borne transmission of contaminated air is the second most prevalent cause of causing disease for patients, healthcare workers, and visitors. The role of the ACMV system in hospitals is more vital than just the provision of thermal comfort. In many cases, proper air-conditioning is a factor of paramount importance in patient therapy and in some cases, it is the major treatment. The quality of the overall hospital environment depends on control of certain factors like pressure, temperature, velocity, and indoor air quality. These variables are analyzed using the Computational Fluid Dynamics technique. The role of CFD is important in the prediction of

ventilation performance in buildings. The isolation room should maintain negative air pressure with respect to the surroundings. The negative pressure is maintained by extracting a higher amount of air than that is supplied (Fig:1). This pressure differential causes air to flow into the room through various leakage areas (e.g. the perimeter of doors and windows, utility/fixture penetrations, cracks, etc.) instead of the air flowing outwards.

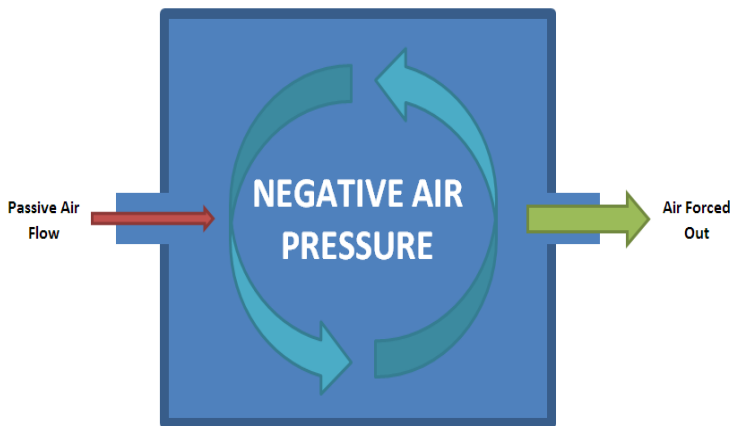


**Fig: 1** physics for this case  
Source: wikipedia

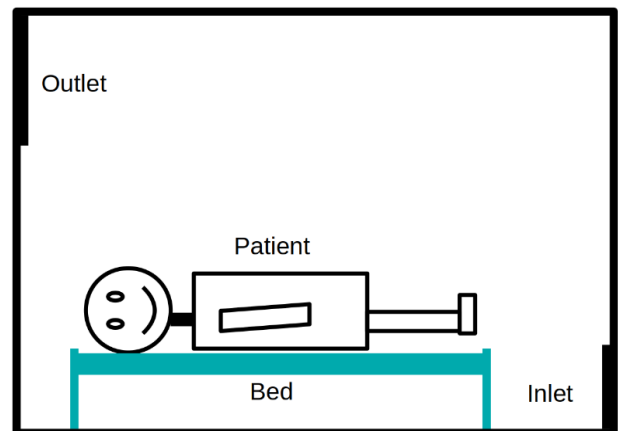


**Fig: 2** rough geometry for this case

### Literature review:

**Prasad Mahajan et al. [1]** Airflow Simulation of an Isolation room using CFD Technique. They analyzed the steady-state conditions of the room. By plotting contours of temperature, velocity, pressure, and  $CO_2$  concentration various conclusions are Made. The simulation was performed using Ansys Fluent numerical model is based upon finite volume. **Shih Y.C. et al. [2]** studied the dynamic airflow simulation within an isolation room. They analyzed the effects of a moving person on the indoor air distribution including velocity, pressure, and contaminant fields. CFD simulation involved the use of dynamic meshing and transient setup. K- $\epsilon$  turbulence model and  $CO_2$  as a contaminant source was adopted in the simulation. The simulation was performed using Ansys Fluent numerical model is based upon finite volume. **Chow et al. [3]** investigated the ventilation system of a hospital operating theatre and found that the optimum supply air-distribution systems provide the desired effects within the surgical field rather than in the entire room. **Cheong K.W.D et al. [4]** “Development of ventilation design strategy for effective removal of pollutant in the isolation room of a hospital” in this paper they analyzed the airflow and pollutant distribution patterns in a “negative pressure” isolation room by means of CFD modelling based on three ventilation strategies. In all the three ventilation strategies the locations of supply diffusers and extract grilles were changed and numerical simulations performed on these strategies were compared. The aim was to detect which strategy is better for pollutant removal. It was found that Ventilation Strategy 3 is best with pollution removal efficiency values exceeding 1 and it has the lowest exposure level at the three locations. **Guillermo Giraldo [7]** investigated

different outlet positions to reduce the risk of bacteria to be spread in an operation theater room. Case study also considered thermal comfort and fresh air velocity conditions inside the hospital room. In this case, we validate against [7], and moving further, we look at positions of inlet- outlet combination that will be most suitable.

## 2. Problem statement:

In this case, there is a room with an inlet and an outlet along with a patient and a bed. The air is flowing from the inlet to the outlet and to maintain negative pressure inside the room a higher proportion of the air is extracted than that is supplied. Patient is also releasing heat from the body. Thermal comfort near the patient has to be ensured and also pressure inside the room has to be ensured to remain negative always. The main analysis of this case is to find the best suitable position of inlet and outlet and along with this suitable bed position such that it reduces the chances of the infection to other people (doctor, nurse, patient visitors). For this case The flow conditions are shown as in Table 1:

Fluid property	Value
Kinetic viscosity, fluid( $\mu$ ), Pa.s	$1.825 \cdot 10^{-5}$
Reference Density of the fluid( $\rho$ ), kg/m <sup>3</sup>	1
coefficient of thermal expansion, $K^{-1}$	0.0034
Prandtl number	0.7039

**Table 1:** Details of fluids property

## 3. Mathematical modelling:

The initial temperature of the fluid is taken as 295.15K and all the thermophysical properties are taken for 295.15K, the density of air is considered as a variable because it changes by changing the temperature. So to incorporate the variable density, Boussinesq approximation is used, according to this approximation change in density is assumed as a negative linear function of temperature. The approximation is accurate when density variations are small as this reduces the nonlinearity of the problem.

Mathematically,

$$\nabla \rho = -(\rho_0 \beta \Delta T)$$

Where

- $\rho_0$  is the initial density of the fluid
- $\beta$  is the coefficient of thermal expansion
- $\Delta T = T - T_{ref}$
- The above approximation mentioned in the equation is valid only when  $\Delta \rho \ll \rho_0$

### 3.1 Continuity equation:

$$\frac{1}{\rho} \frac{D\rho}{Dt} + \nabla \cdot \mathbf{u} = 0$$

### 3.2 Momentum equation:

In the Boussinesq Approximation, It assumes that variations in density have no effect on the flow field, except that they give rise to buoyancy forces. In more practical terms, this approximation is typically used to model liquids around room temperature, natural ventilation in buildings, or dense gas dispersion in industrial set-ups.

N-S equation for general compressible flow case is :

$$\rho\left(\frac{\partial \rho}{\partial t} + u \cdot \nabla u\right) = -\nabla p + \nabla \cdot \left\{ \mu(\nabla u + (\nabla u)^T) - \frac{2}{3}\mu(\nabla u)I \right\} + \rho g$$

where  $u$  is the fluid velocity,  $p$  is the fluid pressure,  $\rho$  is the fluid density,  $\mu$  is the fluid dynamic viscosity,  $I$  is the identity matrix, and  $g$  is the acceleration due to gravity. The Navier-Stokes equations are solved together with the continuity equation. The Boussinesq approximation states that the density variation is only important in the buoyancy term, and the rest of the term it can treat as constant.

So now NS equation will look like

$$\rho_0\left(\frac{\partial \rho}{\partial t} + u \cdot \nabla u\right) = -\nabla p + \nabla \cdot \left\{ \mu(\nabla u + (\nabla u)^T) - \frac{2}{3}\mu(\nabla u)I \right\} + \rho g$$

where the temperature and pressure-dependent density,  $\rho$ , have been replaced by a constant density,  $\rho_0$ , except in the body force term representing the buoyancy force. From the Boussinesq approximation continuity equation can be rewrite as the incompressible form

$$\nabla \cdot u = 0$$

because the magnitude of  $\frac{1}{\rho} \frac{D\rho}{Dt}$  is small with respect to the velocity gradients  $\nabla \cdot u$

And by neglecting the lower magnitude term NS equation will be

$$\rho_0\left(\frac{\partial \rho}{\partial t} + u \cdot \nabla u\right) = -\nabla p + \mu(\nabla^2 u) + \rho g$$

And it also can rewrite as

$$\rho_0\left(\frac{\partial \rho}{\partial t} + u \cdot \nabla u\right) = -\nabla p + \mu(\nabla^2 u) + (\rho_0 + \Delta\rho)g$$

Further by changing the density in terms of temperature

$$\rho_0\left(\frac{\partial \rho}{\partial t} + u \cdot \nabla u\right) = -\nabla p + \mu(\nabla^2 u) + \rho_0 g - \frac{\rho_0(T-T_0)}{T_0} g$$

And  $p = P - \rho_0 g h$

x-Momentum:

$$\rho_0 \nabla \cdot (uu) = -\nabla P + \nabla \cdot (\mu \nabla u) + [\rho_0 - \rho_0 \beta (T - T_{ref})]$$

$$\nabla \cdot (uu) = -\nabla \bar{p} + \mathfrak{G}_{eff} \nabla^2 u + \rho_k g$$

$$\rho_k = 1 - \beta (T - T_{ref})$$

Where,

$\rho_k$  effective kinematic density.

y-Momentum:

$$\rho_0 \nabla \cdot (vv) = -\nabla P + \nabla \cdot (\mu \nabla v) + [\rho_0 - \rho_0 \beta (T - T_{ref})]$$

$$\nabla \cdot (vv) = -\nabla \bar{p} + \mathfrak{G}_{eff} \nabla^2 v + \rho_k g$$

z-Momentum:

$$\rho_0 \nabla \cdot (ww) = -\nabla P + \nabla \cdot (\mu \nabla w) + [\rho_0 - \rho_0 \beta (T - T_{ref})]$$

$$\nabla \cdot (ww) = -\nabla \bar{p} + \mathfrak{G}_{eff} \nabla^2 w + \rho_k g$$

### 3.4 Energy equation:

$$\nabla(Tu) = \alpha_{eff} \nabla^2 T$$

$$\alpha_{eff} = \frac{\nu}{Pr} + \frac{\nu_t}{Pr_t}$$

Where

$\nu$  is kinematic viscosity

$Pr_t$  turbulent Prandtl number

$\alpha_{eff}$  effective thermal diffusivity

### TURBULENT PROPERTY

Turbulence is a highly transient phenomenon, characterized by a wide range of eddy sizes. So here it is not possible to solve all those eddies numerically and obtain a full profile of the turbulent flow field. So a proper turbulence model is required to solve this issue. Here k- $\epsilon$  turbulence model is used. An important feature in turbulence modeling is averaging (like RAS, which is used in this case), which simplifies the solution of the governing equations of turbulence.

## Model equations for k-ε

The *turbulent kinetic energy* equation,  $k$

$$\frac{D}{Dt}(\rho k) = \nabla \cdot (\rho D_k \nabla k) + P - \rho \varepsilon$$

Where ,

$k$  = Turbulent kinetic energy,

$D_k$  = Effective diffusivity for  $k$ ,

$P$  = Turbulent kinetic energy production rate ,

$\varepsilon$  =Turbulent kinetic energy dissipation rate,

The *turbulent kinetic energy dissipation rate* equation,  $\varepsilon$

$$\frac{D}{Dt}(\rho \varepsilon) = \nabla \cdot (\rho D_\varepsilon \nabla \varepsilon) + \frac{C_1 \varepsilon}{k} (P + C_3 \frac{2}{3} k \nabla \cdot u) - C_2 \rho \frac{\varepsilon^2}{k}$$

where,

$D_\varepsilon$  = Effective diffusivity for  $\varepsilon$

$C_1, C_2$  = Model coefficient

The *turbulent viscosity* equation,  $\nu_t$

$$\nu_t = C_\mu \frac{k^2}{\varepsilon}$$

Where,

$C_\mu$  = Model coefficient for the turbulent viscosity,

$\nu_t$  = Turbulent viscosity,

## 4. Simulation procedure:

The case deals with 3D turbulent airflow simulation within a negative pressure ventilation room. First, a tutorial case of buoyantPimpleFoam is copied from the tutorial folder and pasted in the desired folder. Then all required input parameters are set before starting the simulation. Also, the blockMeshdict and snappyHexMeshdict files are to be modified as per requirement. A **buoyantPimpleFoam** solver is to be used to run the simulation.

### 4.1 Creating geometry & Mesh :

#### ➤ Geometry

Room geometry with inlet and outlet is done by using blockMesh. The dimension of the room is  $4*4*2.6\text{ m}^3$ . And for creating the patient and bed model Solidworks software is used. The dimension & geometry of the isolation room, patient bed are given below:

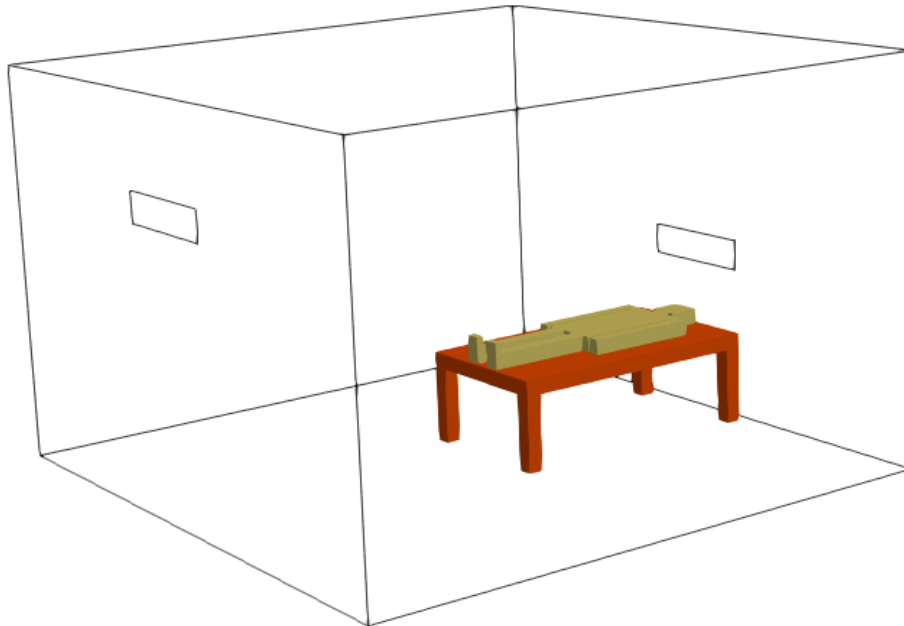


**Fig. 3:** Geometry of isolation room with bed and patient.

Name	X-direction length (m)	Y-direction width (m)	Z-direction Height (m)
Room	4	4	2.6
Bed	1	1.75	0.6
Bed-leg1	0.1	0.1	0.5
Bed-leg2	0.1	0.1	0.5
Bed-leg3	0.1	0.1	0.5
Bed-leg4	0.1	0.1	0.5
Inlet	0.8	0	0.2
Outlet	0.8	0	0.2

**Table 2:** Dimensions of an isolation room & bed

Name	X-direction length (m)	Y-direction width (m)	Z-direction Height (m)
------	------------------------	-----------------------	------------------------

Body	0.6	0.75	0.1
Head	0.2	0.2	0.1
Hand	0.1	0.75	0.1
Leg	0.1	0.7	0.1

**Table 3:** Dimensions of patient

### ➤ Mesh:

The case directories 0, constant, system are created with appropriate sub-directories. The .stl file in the triSurface directory which itself is in the constant directory. The system directory consists of dictionaries like blockMeshDict, snappyHexMeshDict, surfaceFeatureExtractDict.

### blockMesh:

The room size 4m\*4m\*2.6m is designed by the blockMeshDict utility which consists of 9 blocks and simpleGrading (1 1 1) is used to keep aspect ratio near about 1.

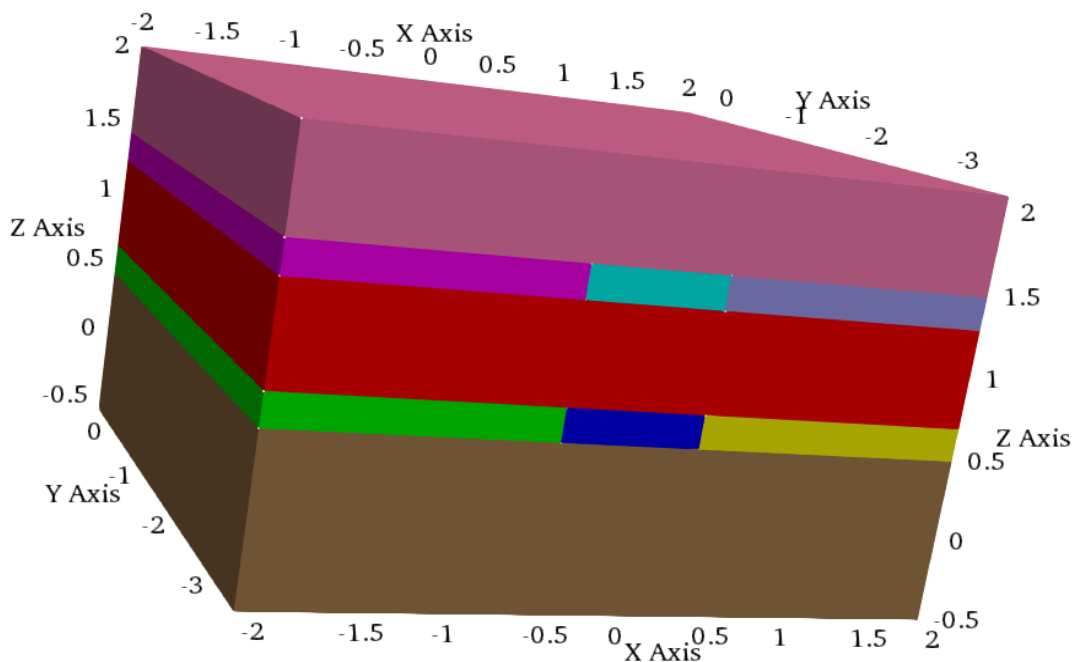


**Fig 4 :** blocks

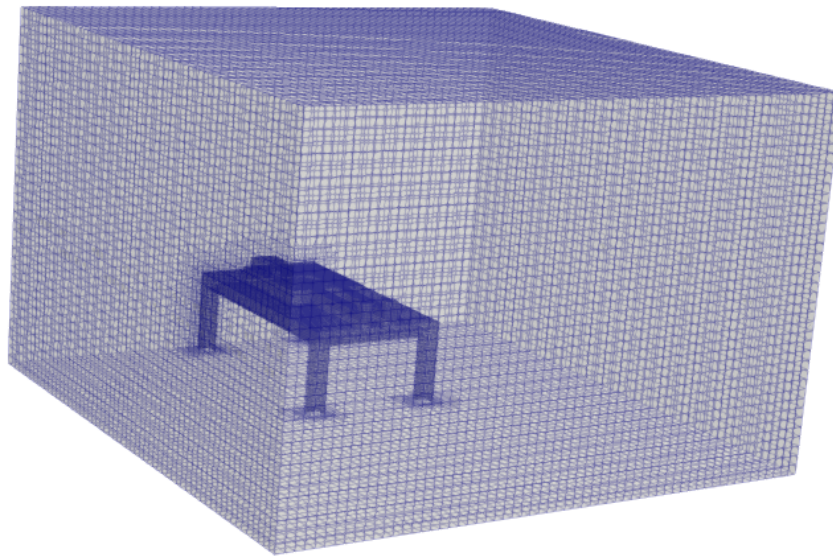


**Figure 5:** Domain and blockMesh

### The snappyHexMeshDict:

The snappyHexMesh is used with the surfaceFeatureExtract utility to mesh the underlying model by following operations:

- 1) The edges are extracted from the .stl files (bed.stl, patient.stl) through the surfaceExtractFeature and are stored as bed.eMesh and patient.eMesh in the triSurface directory. To run the feature, the surfaceFeatureExtractDict is specified with the .stl files to operate and the settings are tuned to extract all the edges in the .stl files.
- 2) The domain detects the model and uses castellated Mesh to coarsely remove the blocks that are contained within the model's outline. This is further refined upto the level specified. The refinement surface is set to the eMesh generated, to detect the edges, through which the castellated mesh is generated upon.
- 3) The snappyHexMesh dictionary is set with refinements of level 2 to capture intricacies near the bed and the patient.

Edge refinement level	2
Surface refinement level	(2 2)

**Table 4:** SnappyHexMesh refinement

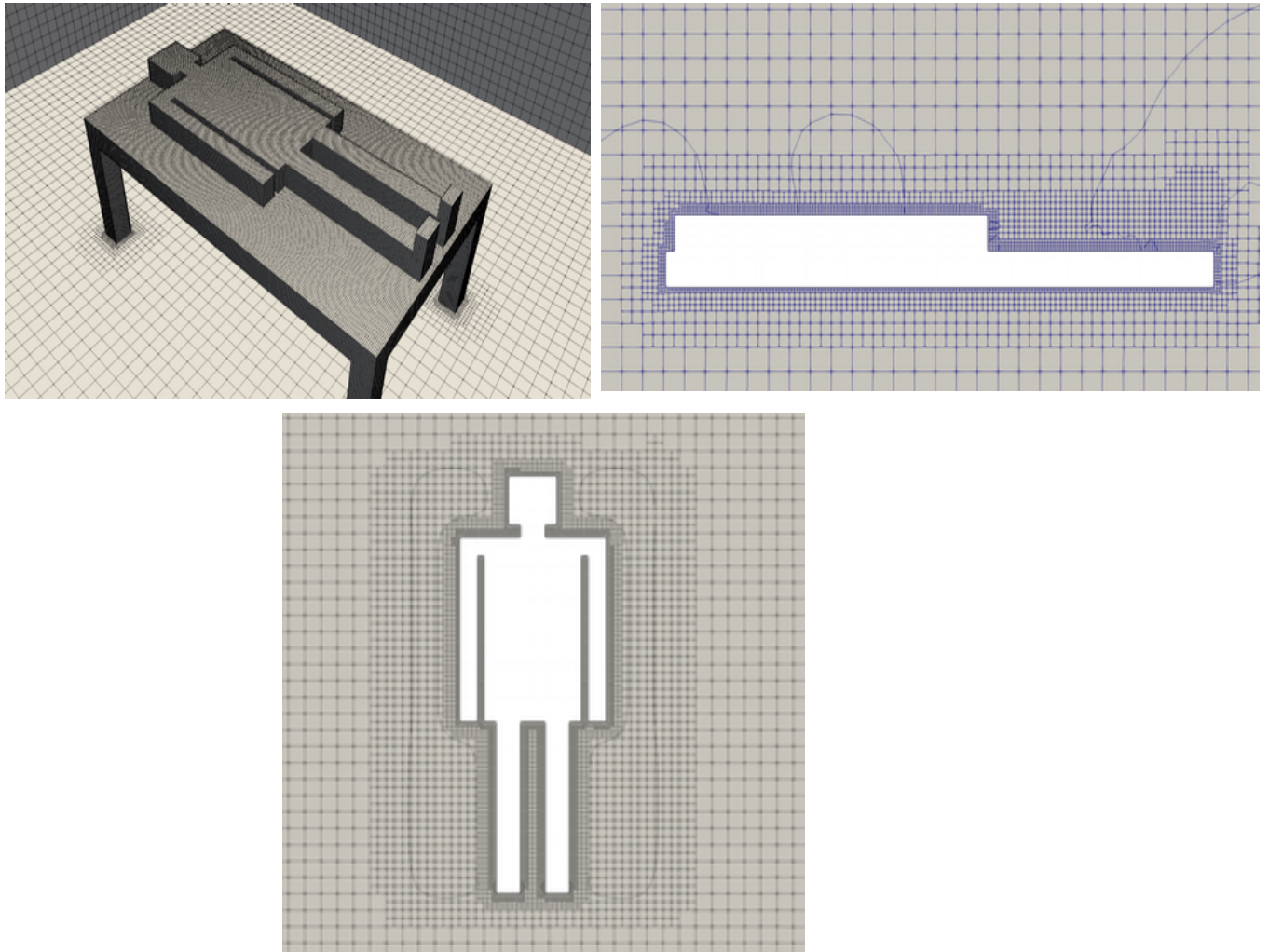


**figure 5:** Refined Mesh

**checkMesh:** The mesh is generated and the checkMesh command is run to locate illegal faces of the mesh, if any. The result returned as MESH OK.

Domain	(-2 -3.4 -0.6) (2 0.6 2)
Points	249970
Faces	685635
Internal faces	647373
Cells	217903
Faces per cells	6.11744
Boundary patch	5
Max skewness	1.33146
Max. Aspect ratio	2.72146

**Table 5:** CheckMesh data

## 4.2 Initial and Boundary Conditions

There are a total of eight files in the '0' folder. Out of these, four files are for turbulence modelling and the other four files are P\_rgh(static pressure), P, T and U.

Boundary	U	P	P_rgh	T
<b>inlet</b>	zeroGradient	calculated	totalPressure $P_0 = 4.5 * 10^{-5}$	fixedValue(295.15K)
<b>outlet</b>	zeroGradient	calculated	fixedValue(-8/-11Pa)	zeroGradient
<b>bed</b>	noSlip	calculated	fixedFluxPressure	zeroGradient
<b>patient</b>	noSlip	calculated	fixedFluxPressure	externalWallHeatFluxTemperature flux( $56.52\text{W}/\text{m}^2$ )
<b>wall</b>	noSlip	calculated	fixedFluxPressure	zeroGradient

**Table 6:** Boundary Condition

## 4.3 Solver

The solver used is “buoyantPimpleFoam”. This is transient solver for buoyant, turbulent flow of compressible fluids for ventilation and heat-transfer. Here Boussinesq approximation is used by changing the equationOfState to Boussinesq in the “thermoPhysicalProperties” file located in “constant” folder to use this solver for the incompressible fluid. The PIMPLE Algorithm is a combination of PISO (Pressure Implicit with Splitting of Operator) and SIMPLE (Semi- Implicit Method for Pressure-Linked Equations). All these algorithms are iterative solvers but PISO and PIMPLE are both used for transient cases whereas SIMPLE is used for steady-state cases. In OpenFoam v-7 “buoyantBoussinesqPimpleFOAM” solver is combined with “buoyantPimpleFoam” solver but approximation can be implemented. Here thermophysical property(thermo type) are shown below for this case to incorporate Boussinesq approximation in this buoyantPimpleFoam solver (for use this solver for a incompressible fluid )

type	heRhoThermo
mixture	pureMixture
transport	const
thermo	eConst
equationOfState	Boussinesq
specie	specie
energy	sensibleInternalEnergy

**Table 7:**thermoType

## 4.4 Post-processing

The paraview software can be used to visualize the simulation results in OpenFOAM. This can be run by typing the *paraFoam* command line in the terminal to open the paraview software and upload the case.

## 5. Results

Ensuring negative pressure inside the whole domain is our foremost priority for which numerous experiments have been conducted to find the most suitable inlet and outlet position so that the chance of the infection of the other people (like doctor, nurse) will be less. So for this, three case studies were performed with different inlet and outlet positions (outlet static pressure -8pa)

**Case-1: Validation case**

**Case-2: Perpendicular inlet-outlet arrangement**

**Case-3: Parallel inlet-outlet arrangement**

**Case-4: Improvised solution**

**Case-1: Validation case**

Initially, a referenced case is converted into an OpenFoam case. For that, the same positions of inlet outlets with exact same dimensions are used. Boundary conditions are kept the same and results are analyzed as shown below. Reference paper analyzed is from *Airflow Simulation of an Isolation room using CFD Technique*. [1]

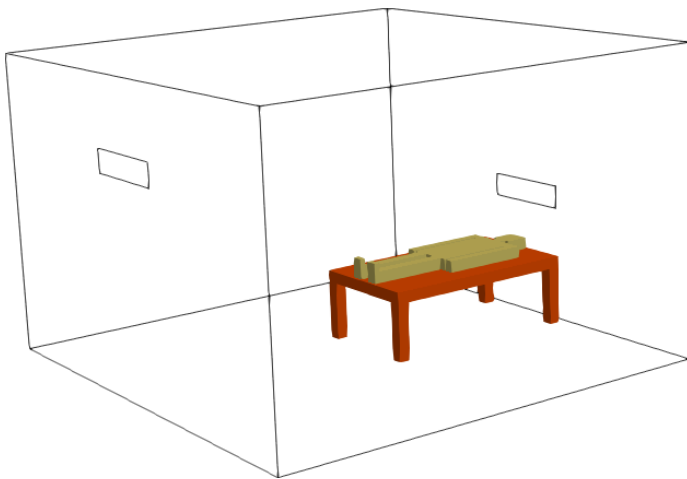


Fig 6: validation case arrangement

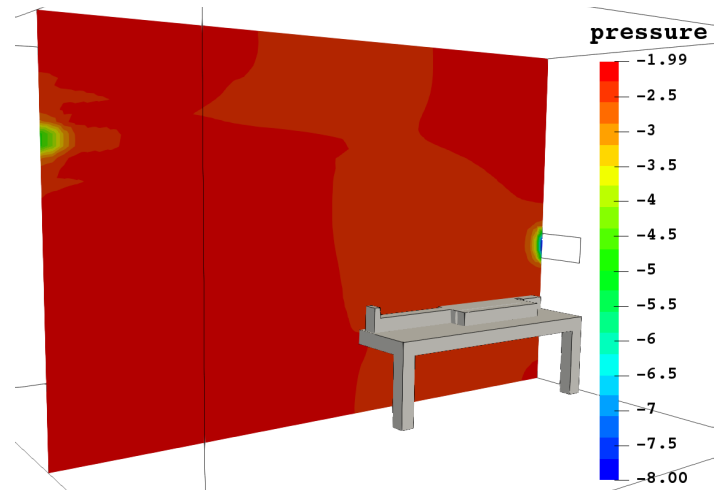


Fig 7: validation case pressure contour

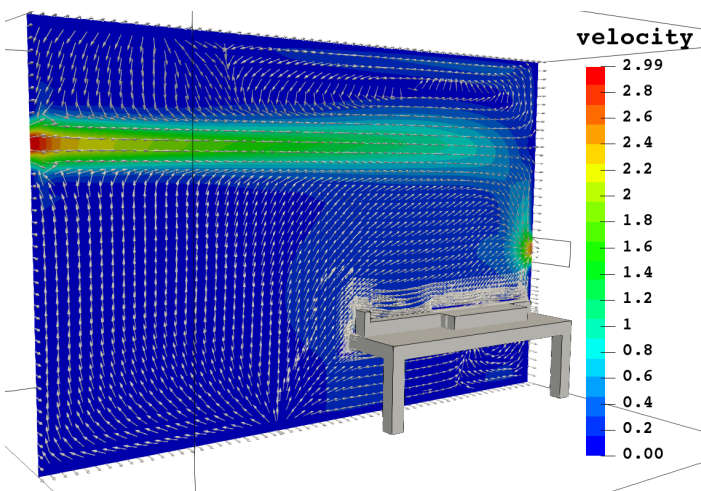


Fig 8: validation case velocity contour & glyph

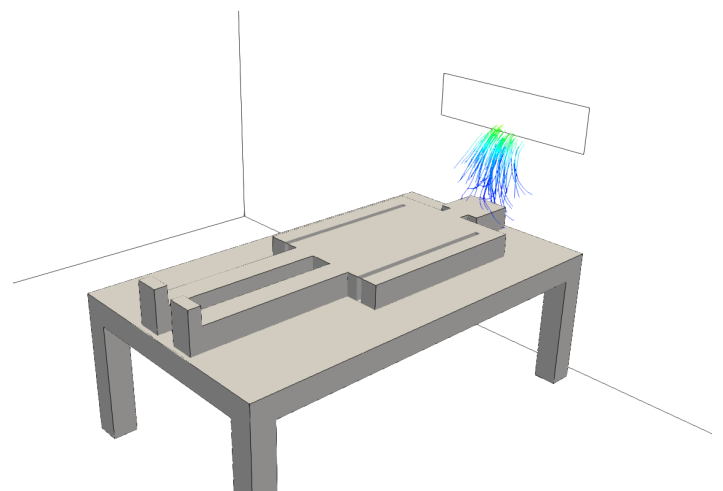


Fig 9: validation case streamline

**Case-2: Perpendicular inlet-outlet arrangement**

Additionally an perpendicular inlet-outlet arrangement is kept with the same dimensions of the domain. Boundary and Initial conditions kept the same and pressure-velocity contours are analyzed as shown below. Velocity vector glyph and streamlines are shown in the figure.

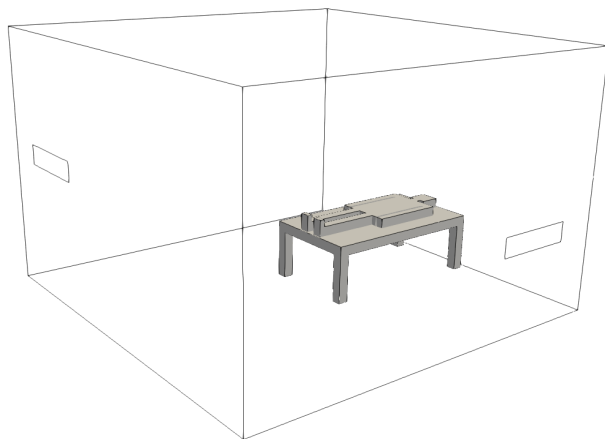


Fig 10: perpendicular inlet-outlet case arrangement

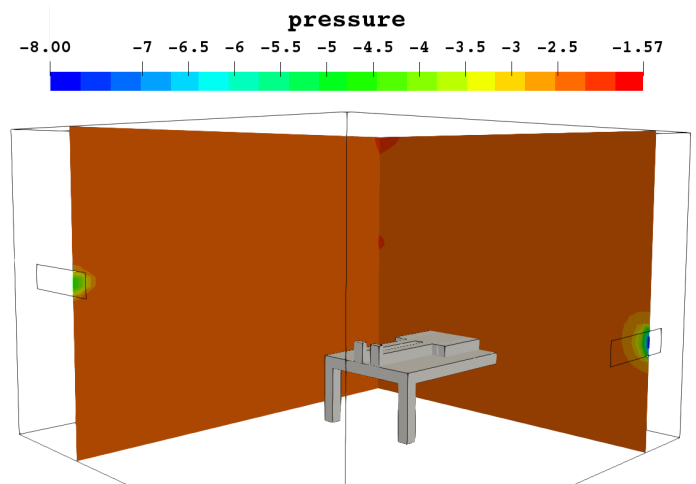


Fig 11: perpendicular inlet-outlet pressure contour

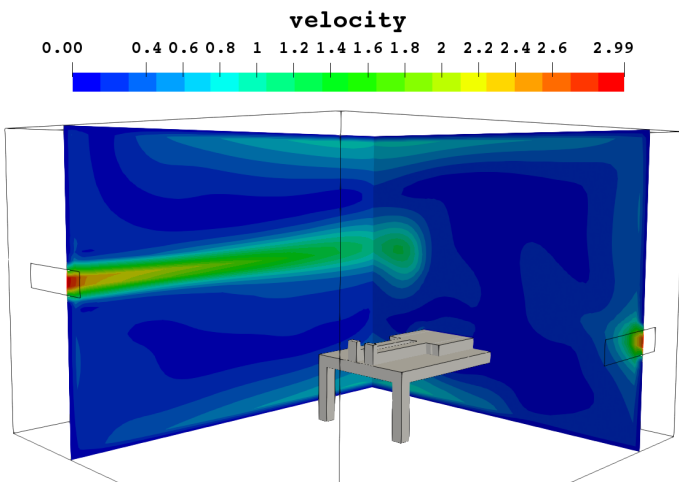


Fig 12: perpendicular inlet-outlet case velocity contour & glyph

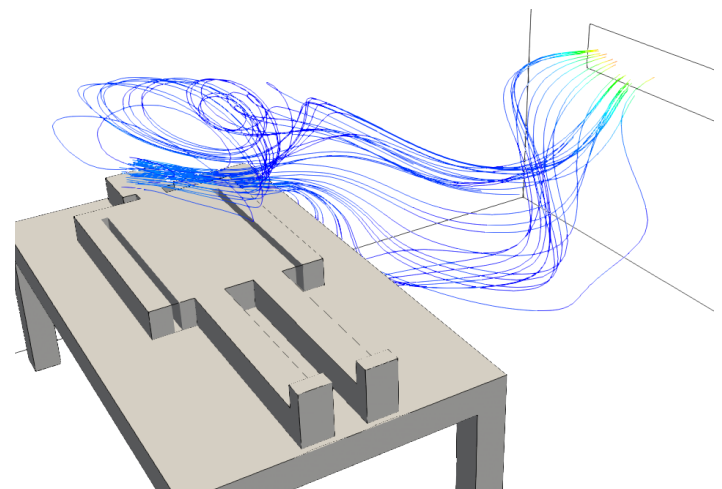


Fig 13: perpendicular inlet-outlet case streamline

**Case-3: Parallel inlet-outlet arrangement**

Third different inlet outlet position arrangement is shown below in the figure. Results show improvement of air circulation near to the face of the patient. But still there is a scope of improvisation in the case because of the gap in between patient and outlet.

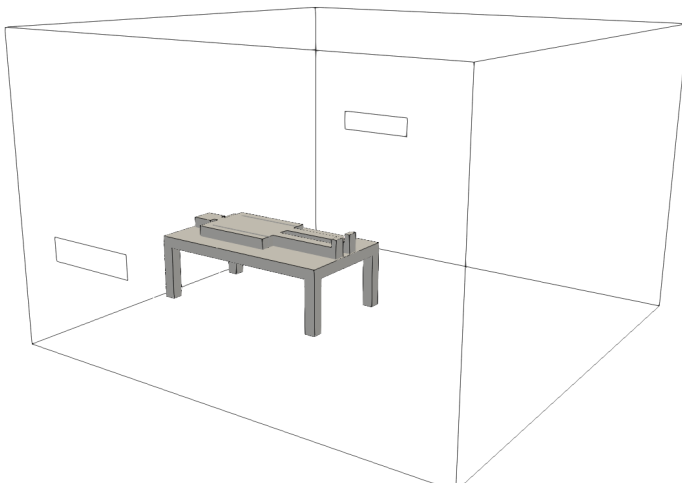


Fig 14: parallel inlet-outlet case arrangement

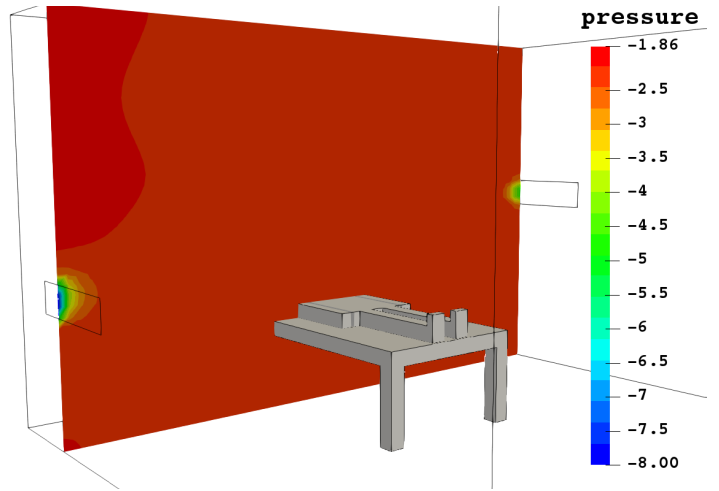


Fig 15: parallel inlet-outlet case pressure contour

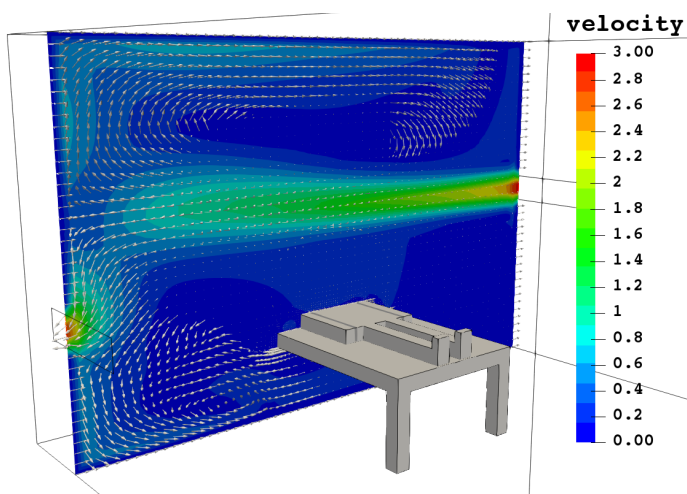


Fig 16: parallel inlet-outlet case velocity contour & glyph

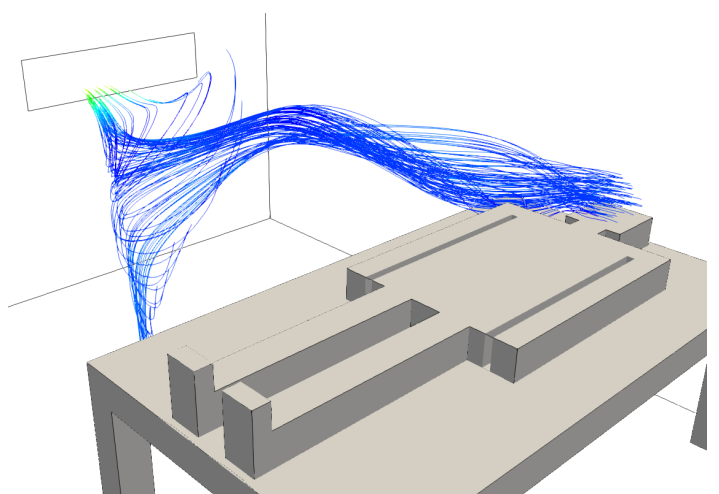


Fig 17: parallel inlet-outlet case streamline

**Case-4: Improvised solution**

From the above three cases it is observed that the best suitable position of outlet is right above the patient. For better circulation of air near to the patient’s head, more negative pressure is applied to the outlet patch. Results show the best outcome of all previous cases.

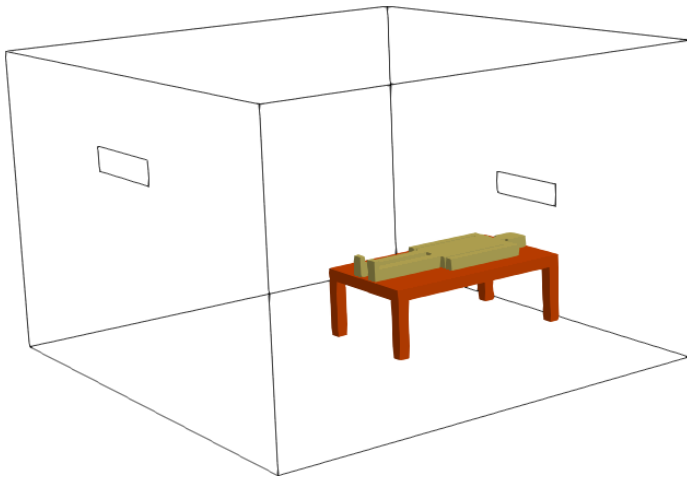


Fig 18: improved case arrangement

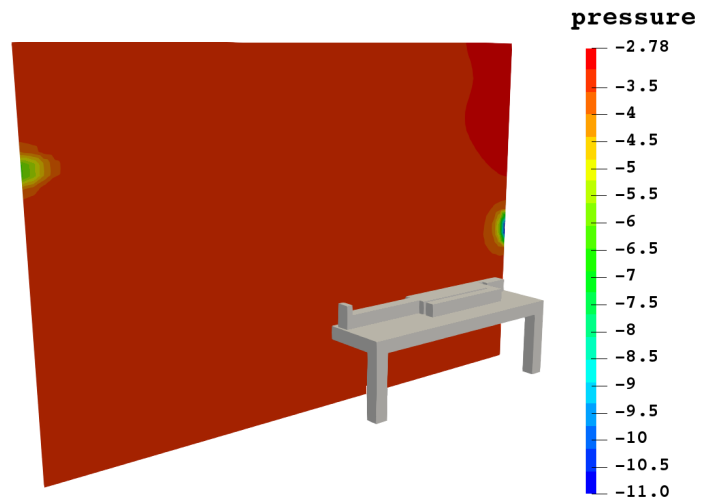


Fig 19: improved case pressure contour

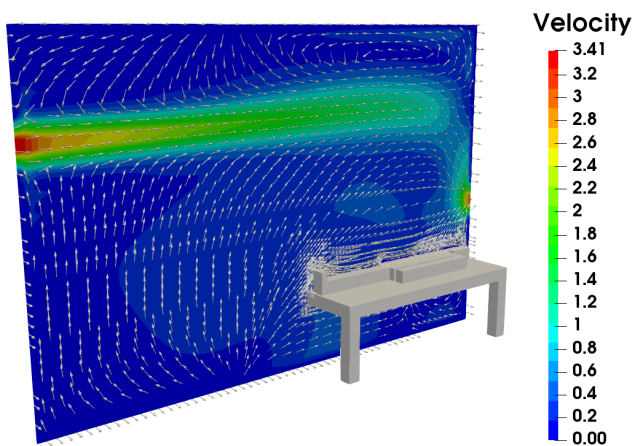


Fig 20: improved case velocity contour & glyph

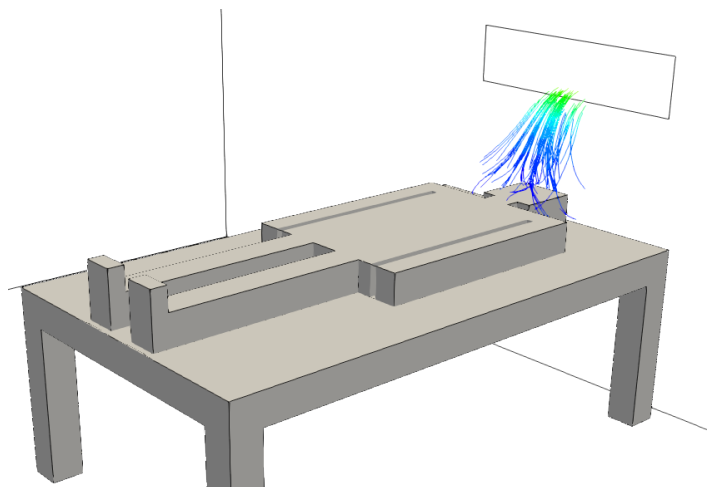


Fig 21: improved case streamline

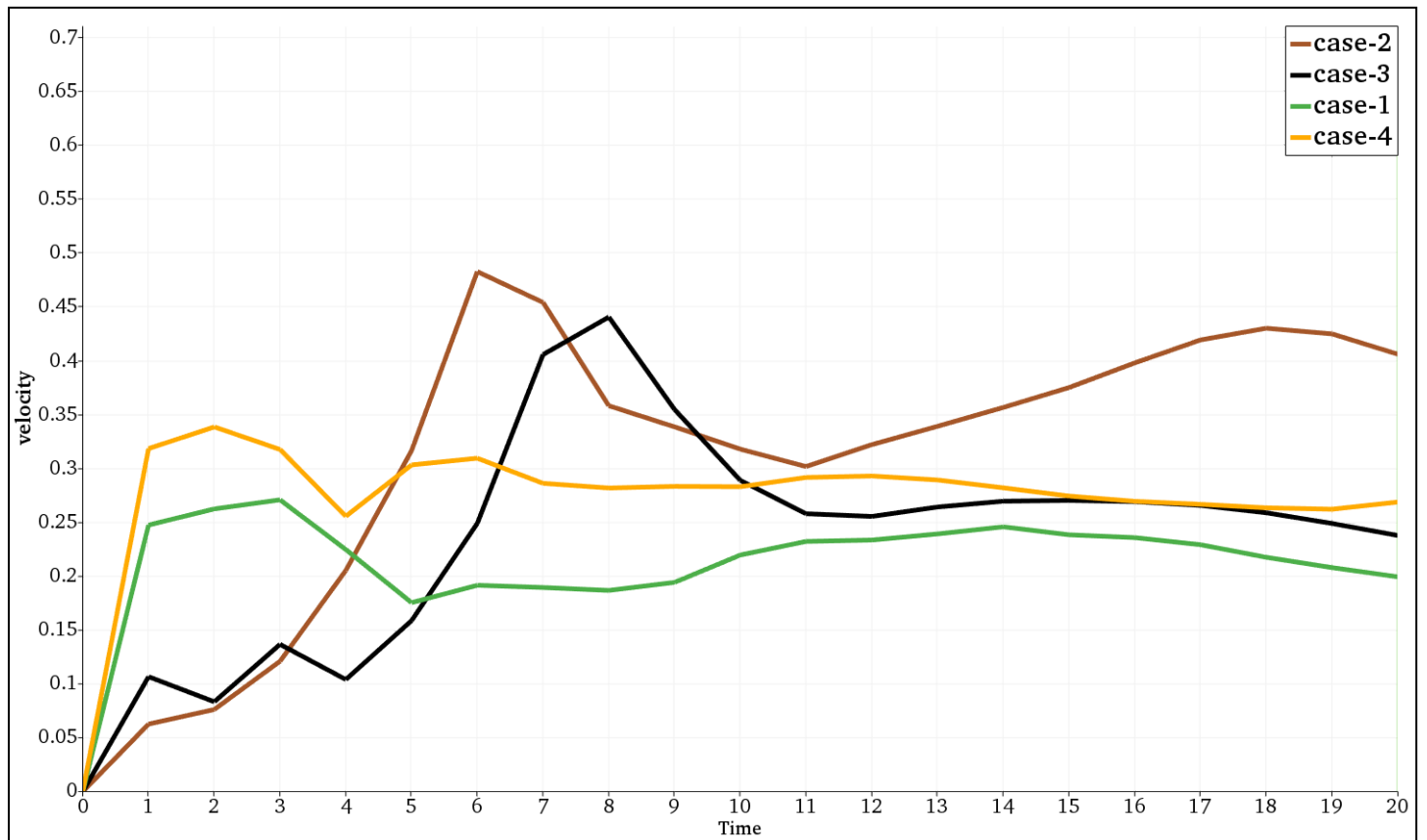
**Velocity near to the patient's head vs time:**

Fig 22: velocity vs time near to the patient's head

## 6. Conclusion

The focus of this study was to investigate the best inlet-outlet combination for a negative pressure room. First a validation exercise was carried out against reference [7]. Following this different inlet-outlet configurations were tested. From the analysis of the pressure and velocity contours, it is hereby concluded that the best suitable position for inlet and outlet is “Inlet is in the leg side of the patient, outlet is in the head side of the patient” - this position of the room is inherently better than the others due to the fact that the outlet is very near to the bed and hence most of the air which passes over the patient’s face goes out of the room through the outlet and there is a very small chance that infected air over the patient’s face spreads throughout the entire room. On the other hand for the remaining cases, if any health-care worker (including doctors) stand in between the bed and the outlet then there is a chance of infection of that person due to the contaminated air. That issue can be solved by shifting the bed position near the outlet.

It has also been determined that the most comfortable velocity of  $< 0.2$  m/s ([7]) is satisfied in our simulation case-1, case-3 & case-4.

## Reference

- [1]. Prasad Mahajan, Arun Saco S, R. Dinesh Kumar, Thundil Karuppa Raj R. Airflow Simulation of an Isolation room using CFD Technique, Volume 118 No. 18 2018, 4261-4269
- [2]. Shih, Y.C., Chiu, C.C., and Wang, O., 2007. Dynamic airflow simulation within an isolation room. *Building and Environment*, 42, 3194-3209.
- [3]. Chow TT, Ward S, Liu JP, Chan FCK. Airflow in hospital operating theatre—the Hong Kong experience. *Proceedings of healthy buildings 2000—design and operation of HVAC systems*, vol. 2. 2000, p. 419–24.
- [4]. Cheong, K.W.D., and Phua S.Y., 2006. Development of ventilation design strategy for effective removal of pollutant in the isolation room of a hospital. *Building and Environment*, 41, 1161-1170.
- [5] OpenFOAM User Guide, Version 7
- [6] <https://www.comsol.co.in/multiphysics/boussinesq-approximation>
- [7] <https://www.simscale.com/blog/2018/12/cfd-airflow-operating-room/>
- [8] [https://en.wikipedia.org/wiki/Thermal\\_comfort#Elevated\\_air\\_speed\\_method](https://en.wikipedia.org/wiki/Thermal_comfort#Elevated_air_speed_method)

# CFD study of deLaval nozzle with Fanno and Rayleigh condition

Shouvik ghorui

Jadavpur University

## Abstract

**Computational fluid dynamics (CFD)** is a branch of fluid mechanics that uses numerical analysis and algorithms to solve fluid flow problems. The objective of the current study is to study the variation of flow parameters like pressure, temperature and Mach number by adding friction & heat transfer to a converging-diverging nozzle with the help of CFD. At first, a comparative study is done with an already published paper (only trend of the graph is matched in the subsonic regime) and then a new contribution has been added. The mesh is done using the *blockMesh* utility of OpenFoam. Also this paper describes implementation of heat-flux and friction in OpenFoam. Widely used k-epsilon turbulence model with wall function treatment at wall boundary used. Discretized conservation equations like continuity, momentum, energy and turbulence are solved simultaneously using CFD Open Source package **OpenFOAM® V-7.0** with *rhoCentralFoam* solver to simulate the flow Physics.

**Keywords:-** CFD, OpenFOAM, CD Nozzle, Fanno flow, Rayleigh flow.

## 1. Introduction

Convergent-Divergent (CD) supersonic nozzles are significantly used for high-speed missiles and rocket nozzles. From the design point of view, a nozzle is considered to be a pipe with varying cross-sectional areas throughout the length. CD Nozzle is a very interesting topic because of its dual nature (If the flow reaches sonic condition at the throat, then only the velocity will increase at the diverging section and if the flow does not reach the sonic condition at the throat, then at the diverging section velocity will decrease). In this case study, our aim is to see the effect of the pressure, Mach number, temperature by adding heat transfer and friction (Fanno and Rayleigh condition) to the CD Nozzle.

- **Fanno flow** is the adiabatic flow through a constant area duct where the effect of friction is considered. Compressibility effects often come into consideration, although the Fanno flow model certainly also applies to incompressible flow. For this model, the duct area remains constant, the flow is assumed to be steady and one-dimensional, and no heat is added within the duct. The Fanno flow model is considered an irreversible process due to viscous effects.

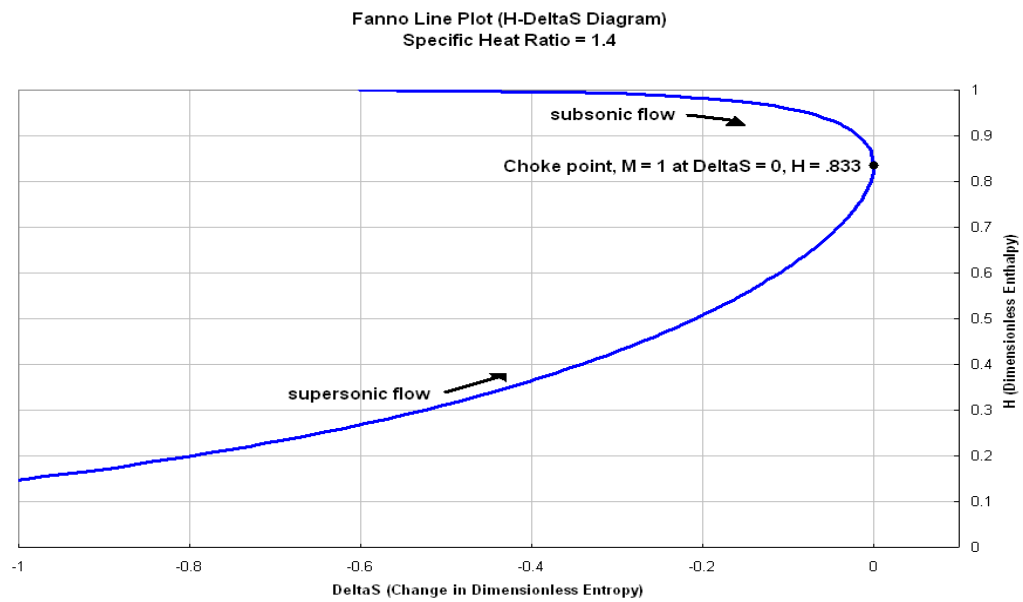


**Fig:1** A Fanno Line is plotted on the dimensionless H- $\Delta S$  axis.

Source: Wikipedia

- **Rayleigh flow** refers to frictionless, non-Adiabatic flow through a constant area duct where the effect of heat addition or rejection is considered. Compressibility effects often come into consideration, although the Rayleigh flow model certainly also applies to incompressible flow. For this model, the duct area remains constant and no mass is added within the duct.

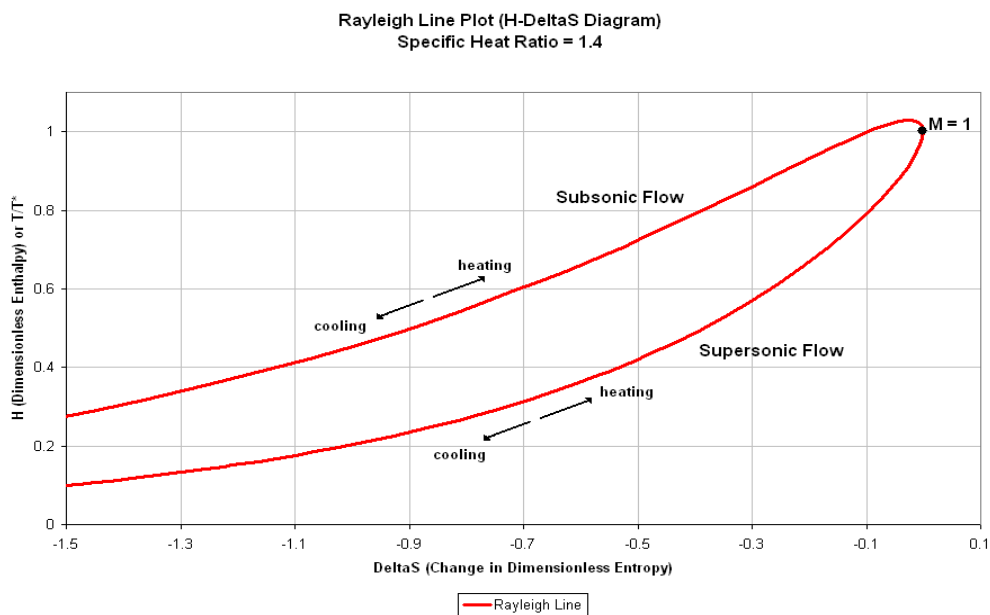


**Fig:2** A Rayleigh Line is plotted on the dimensionless H- $\Delta S$  axis.

Source: Wikipedia

## Literature review:

There are many literatures available on the CD nozzle shape, back pressure etc. But there is a lack of available literature on the CD nozzle with friction and heat flux.

**Alak Bandyopadhyay *et al.*** [1] Modeling of Compressible Flow with Friction and Heat Transfer using the Generalized Fluid System Simulation Program (GFSSP). In this case study, they used two types of geometry (a) a straight pipe of constant diameter, and (b) a converging-diverging nozzle of linearly varying diameter. The effect of friction and heat transfer on the pressure, temperature and Mach no. were studied using these two geometries.

**Ashley Melvin** [2] Flow through a Convergent-Divergent Nozzle. In this case study, he used NASA CFD benchmark case's geometry [3]. He simulated for 3 different exit conditions.

- $p_{\text{exit}} = 1600$  Pa. Isentropic Expansion from Subsonic to Supersonic Speeds.
- $p_{\text{exit}} = 8900$  Pa. Isentropic Subsonic Flow.
- $p_{\text{exit}} = 7500$  Pa. Supersonic Flow with a Normal Shock.

In this case, to test the validity of our solver, we first validated against [1] the constant pipe case. Then we performed case studies on our own geometry (reference from [2]) and also compared the trends of the graph with the nozzle flow of paper for the subsonic condition. After a reasonable agreement between the two, we went forward and extended our case to supersonic flow and supersonic flow with shock.

## 2. Problem statement:

In this case study, NASA benchmark case study [3] geometry along with its pressure and velocity boundary condition is used. And temperature boundary condition is modified to incorporate the heat flux. And k- $\epsilon$  turbulence model is used to incorporate the skin friction.

In this case, we have done four different cases,

Namely {all the nomenclature is given based on **Ashley Melvin** [2] case}:

Case No.	Description
<b>1. Validation case</b>	
1.1.	Fanno Flow-flow with friction in an adiabatic constant area pipe.
1.2.	Rayleigh Flow-flow with heat transfer in a frictionless constant area pipe.
1.3.	Combined Friction and Heat Transfer-Combined Friction and Heat Transfer in a constant area pipe.
<b>2. Subsonic (compare the trends of the graph)</b>	
2.1.	Nothing-flow without friction and heat flux in CD Nozzle (our extended work)

- 2.2. Only\_heat flux-flow with heat transfer in a frictionless CD Nozzle (our extended work)
- 2.3. Only\_friction-flow with friction in an adiabatic CD Nozzle
- 2.4. Combined Friction and Heat Transfer-flow with friction and heat flux in CD Nozzle
  
3. **supersonic** (our extended work)
  - 3.1. Nothing - flow without friction and heat flux in CD Nozzle
  - 3.2. Only\_heat flux - flow with heat transfer in a frictionless CD Nozzle
  - 3.3. Only\_friction - flow with friction in an adiabatic CD Nozzle
  - 3.4. Combined Friction and Heat Transfer - flow with friction and heat flux in CD Nozzle
  
4. **Supersonic with shock** (our extended work )
  - 4.1. Nothing-flow without friction and heat flux in CD Nozzle
  - 4.2. Only\_heat flux-flow with heat transfer in a frictionless CD Nozzle
  - 4.3. Only\_friction-flow with friction in an adiabatic CD Nozzle
  - 4.4. Combined Friction and Heat Transfer -flow with friction and heat flux in CD Nozzle

For this case The flow conditions are shown as in Table 1:

Fluid property	Value
Kinetic viscosity, fluid( $\mu$ ), Pa.s	$1.825 * 10^{-5}$
molWeight ,g/mol	29
Specific Heat ( $C_p$ ), J/kg.K	1005
Prandtl number	1

**Table 1:** Details of fluids property

### 3. Mathematical modelling:

The initial temperature of the fluid is taken as 295.15K and all the thermophysical properties are taken for 295.15K,

#### 3.1 Continuity equation:

$$\frac{1}{\rho} \frac{D\rho}{Dt} + \nabla \cdot u = 0$$

#### 3.2 Momentum equation:

$$\rho \left( \frac{\partial u}{\partial t} + u \cdot \nabla u \right) = - \nabla p + \nabla \cdot \left\{ \mu (\nabla u + (\nabla u)^T) - \frac{2}{3} \mu (\nabla u) I \right\}$$

where  $u$  is the fluid velocity,  $p$  is the fluid pressure,  $\rho$  is the fluid density,  $\mu$  is the fluid dynamic viscosity,  $I$  is the identity matrix

### 3.3 Energy equation:

$$\nabla(Tu) = \alpha_{eff} \nabla^2 T$$

$$\alpha_{eff} = \frac{\nu}{Pr} + \frac{\nu_t}{Pr_t}$$

Where

$\nu$  is kinematic viscosity

$Pr_t$  turbulent Prandtl number

$\alpha_{eff}$  effective thermal diffusivity

#### TURBULENT PROPERTY

Turbulence is a highly transient phenomenon, characterized by a wide range of eddy sizes. So here it is not possible to solve all those eddies numerically and obtain a full profile of the turbulent flow field. So a proper turbulence model is required to solve this issue. Here k- $\epsilon$  turbulence model is used. An important feature in turbulence modelling is averaging (like RAS, which is used in this case), which simplifies the solution of the governing equations of turbulence.

#### Model equations for k- $\epsilon$

*The turbulent kinetic energy equation, k*

$$\frac{D}{Dt}(\rho k) = \nabla \cdot (\rho D_k \nabla k) + P - \rho \epsilon$$

Where,

$k$  = Turbulent kinetic energy,

$D_k$  = Effective diffusivity for  $k$ ,

$P$  = Turbulent kinetic energy production rate,

$\epsilon$  = Turbulent kinetic energy dissipation rate,

*The turbulent kinetic energy dissipation rate equation,  $\epsilon$*

$$\frac{D}{Dt}(\rho \epsilon) = \nabla \cdot (\rho D_\epsilon \nabla \epsilon) + \frac{C_1 \epsilon}{k} (P + C_3 \frac{2}{3} k \nabla \cdot u) - C_2 \rho \frac{\epsilon^2}{k}$$

where,

$D_\epsilon$  = Effective diffusivity for  $\epsilon$

$C_1, C_2$  = Model coefficient

The **turbulent viscosity** equation,  $\nu_t$

$$\nu_t = C_\mu \frac{k^2}{\varepsilon}$$

Where,

$C_\mu$  = Model coefficient for the turbulent viscosity,

$\nu_t$  = Turbulent viscosity,

#### 4. Simulation procedure:

The case deals with 2D turbulent airflow through a deLaval nozzle. First, a tutorial case of rhoCentralFoam is copied from the tutorial folder and pasted in the desired folder. Then all required input parameters are set before starting the simulation. Also, the blockMeshdict file is to be modified as per requirement. A **rhoCentralFoam** solver is to be used to run the simulation.

#### Implement skin friction in OpenFoam :

For implementing skin friction, the “nut” file needs to be modified. Firstly change the Boundary condition of the nozzle wall in the nut file by **nutkRoughWallFunction**. Then put the value of  $K_s$  (Sand – grain roughness height) and  $C_s$  (Roughness constant). Value of  $C_s$  is in between 0 to 1. And  $K_s$  has to be found out from Darcy friction factor by the help of the Moody diagram. For all the cases,  $K_s$  (Sand – grain roughness height) value is 0.03832,  $Re = 10^6$ , darcy friction factor 0.05, relative roughness 0.02.

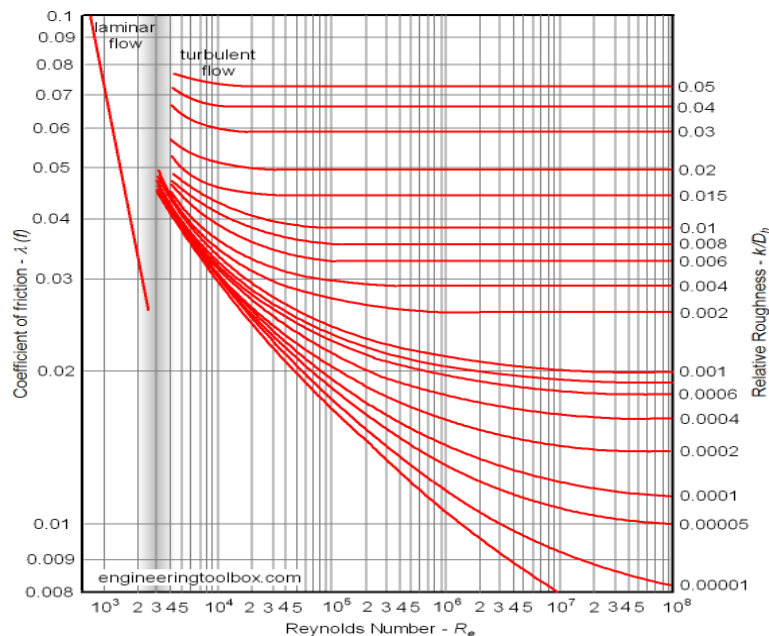


**Fig 3: Moody Diagram**  
Source: engineering toolbox

## Implement Heat Flux in OpenFOAM :

For implementing heat flux from the Nozzle wall externalWallHeatFluxTemperature Boundary condition is used. For this cases value of the heat flux is  $5000 \text{ W/m}^2$  and the official description of the boundary condition is given below:

Property	Description	Required	Default
mode	'power', 'flux' or 'coefficient'	yes	
Q	Power [W]	for mode 'power'	
q	Heat flux [ $\text{W/m}^2$ ]	for mode 'flux'	
h	Heat transfer coefficient [ $\text{W/m}^2/\text{K}$ ]	for mode 'coefficient'	
Ta	Ambient temperature [K]	for mode 'coefficient'	
thicknessLayers	Layer thicknesses [m]	no	
kappaLayers	Layer thermal conductivities [ $\text{W/m/K}$ ]	no	
relaxation	Relaxation for the wall temperature	no	1
emissivity	Surface emissivity for radiative flux to ambient	no	0
qr	Name of the radiative field	no	none
qrRelaxation	Relaxation factor for radiative field	no	1
kappaMethod	Inherited from temperatureCoupledBase	inherited	
kappa	Inherited from temperatureCoupledBase	inherited	

### 4.1 Creating geometry & Mesh :

#### ➤ Geometry

A convergent-divergent nozzle of geometry as shown in fig. 4 is considered For this case The nozzle cross-section varies as -

$$A(x) = \begin{cases} 1.75 - 0.75\cos(0.2x - 1)\pi, & 0 < x \leq 5 \\ 1.25 - 0.25\cos(0.2x - 1)\pi, & 5 < x \leq 10 \end{cases}$$

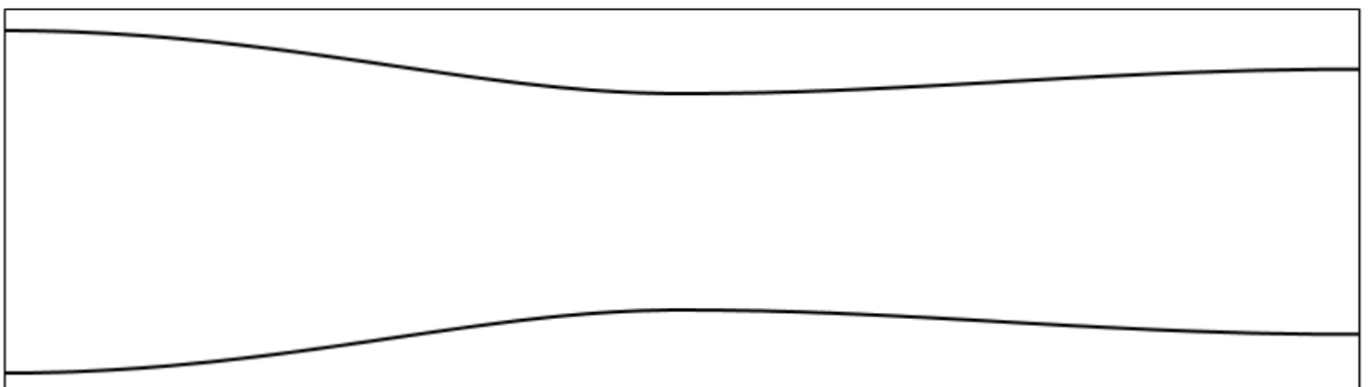


**Fig: 4** The configuration of flow through a convergent-divergent nozzle

### ➤ Mesh

For the meshing purpose, blockMesh utility is used. The geometry is an axisymmetric nozzle, therefore a wedge is considered for the analysis

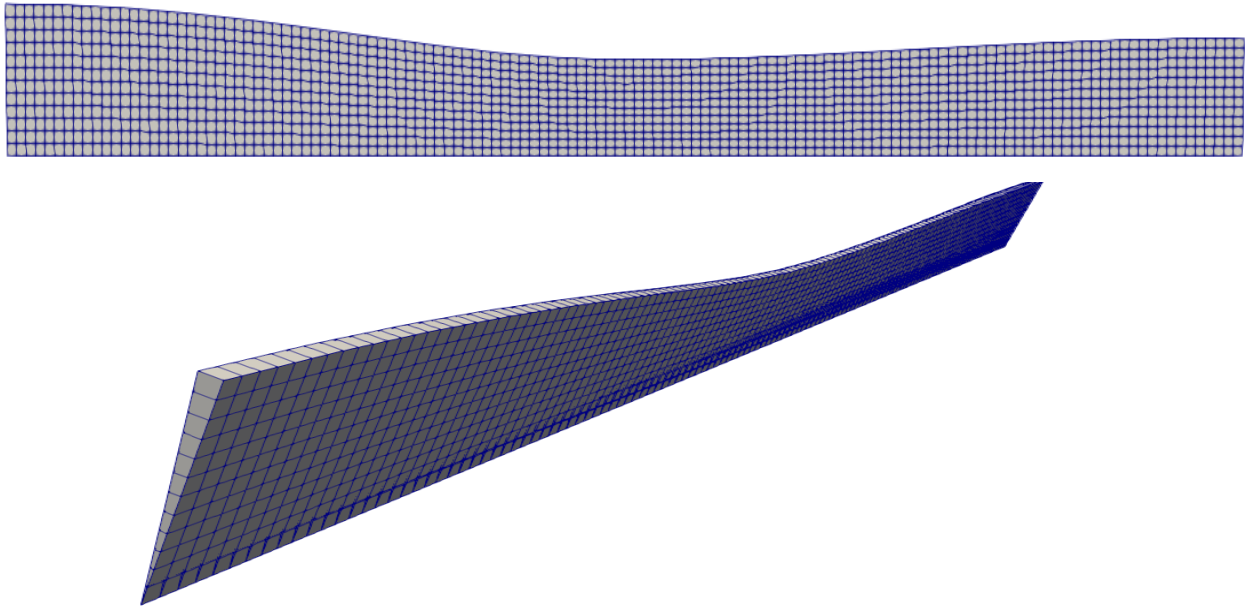


**Fig 5:** Meshing of the wedge.

## 4.2 Initial and Boundary Conditions

There are a total of seven files in the '0' folder. Out of these, four files are for turbulence modelling and the other three files are P, T and U.

In our case studies, whenever we have used friction, we have used a friction factor of 0.05 and whenever we have used heat flux, we have used a heat flux value of  $5000 \text{ W/m}^2$

<b>Case 2 Subsonic</b>		
Pressure	Inlet	10000 Pa
	Nozzle	Zero Gradient
	outlet	8900 Pa
Velocity	Inlet	Zero Gradient
	Nozzle	Slip
	outlet	Zero Gradient
Temperature	Inlet	298 K
	Nozzle	Zero Gradient
	outlet	Zero Gradient

**Table 2:** Subsonic

- For case **2.1**, the boundary condition does not need to change from the above table
- For case **2.2**, Nozzle Temperature BC is to be modified by the code below

```

type          externalWallHeatFluxTemperature
mode          flux;
  q           5000;
thicknessLayers  ();
kappaLayers    ();
kappaMethod    fluidThermo;
value          $internalField;
    
```

- For case **2.3**, Nozzle velocity BC has to be changed from slip to noSlip. And in the nut file the Nozzle BC has to be changed by the code below

```

type          nutkRoughWallFunction;
Ks            uniform 0.03832;
Cs            uniform 0.5;
value          $internalField;
    
```

- For case **2.4**, to add both heat flux & friction, the “nut”, “U”, “T” files have to be modified like the above cases.

<b>Case 3 Supersonic</b>		
Pressure	Inlet	10000 Pa
	Nozzle	Zero Gradient
	outlet	ZeroGradient
Velocity	Inlet	Zero Gradient
	Nozzle	Slip
	outlet	Zero Gradient
Temperature	Inlet	298 K
	Nozzle	Zero Gradient
	outlet	Zero Gradient

**Table 3:** Supersonic

- For case **3.1**, the boundary condition does not need to be changed from the above table but a “setFieldsDict” should be added for the pressure outlet condition and the value of pressure at the outlet region should be 1600.
- The case **3.2,3.3,3.4** are modified as was done earlier

Case 4 Supersonic with shock		
Pressure	Inlet	10000 Pa
	Nozzle	Zero Gradient
	outlet	7500 Pa
Velocity	Inlet	Zero Gradient
	Nozzle	Slip
	outlet	Zero Gradient
Temperature	Inlet	298 K
	Nozzle	Zero Gradient
	outlet	Zero Gradient

**Table 4:** Supersonic

- For case **4.1**, the boundary condition does not need to be changed from the above table
- The cases **4.2,4.3,4.4** have to be modified as was done earlier

### 4.3 Solver

For this case, the most suitable solver is the *rhoCentralFoam* which is a density-based compressible flow solver based on central-upwind schemes of Kurganov and Tadmor. And *rhoCentralFoam* can capture the shock very well. The thermophysical properties of air, assuming perfect gas, is used. The simulation type is turbulent.

## 5. Results

As mentioned earlier, Modeling of Compressible Flow with Friction and Heat Transfer using the Generalized Fluid System Simulation Program (GFSSP) is used for validation. And the results are as shown in the below

## Validation

### Case 1.1 Fanno flow (friction factor 0.002)

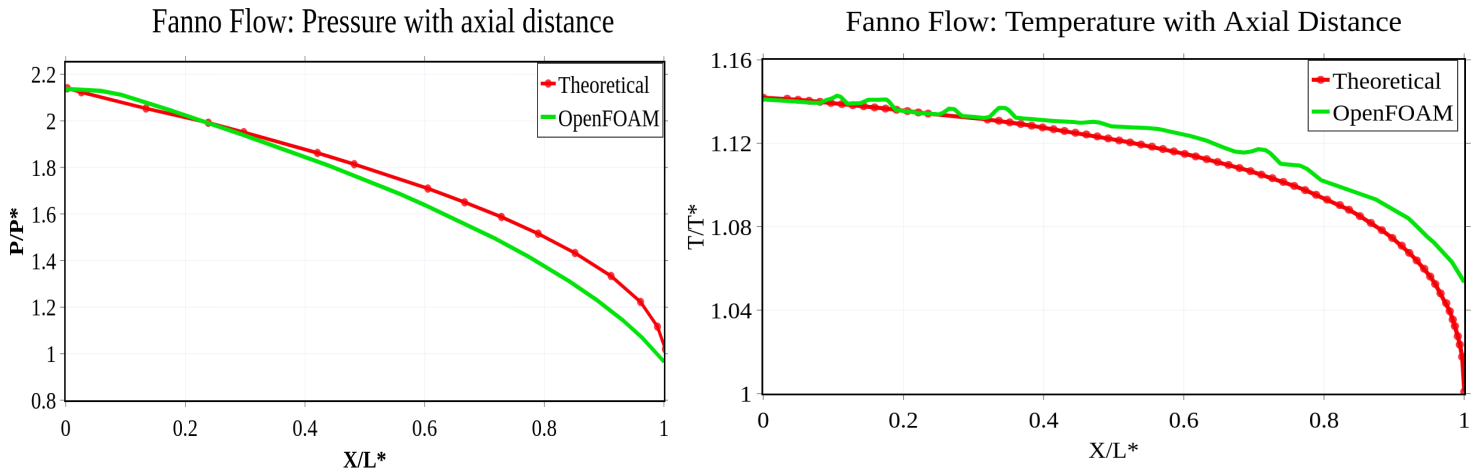


**Fig 6:** Pressure distribution fanno for flow

**Fig 7:** Temperature distribution for fanno flow

### Fanno Flow: Mach No. Plot

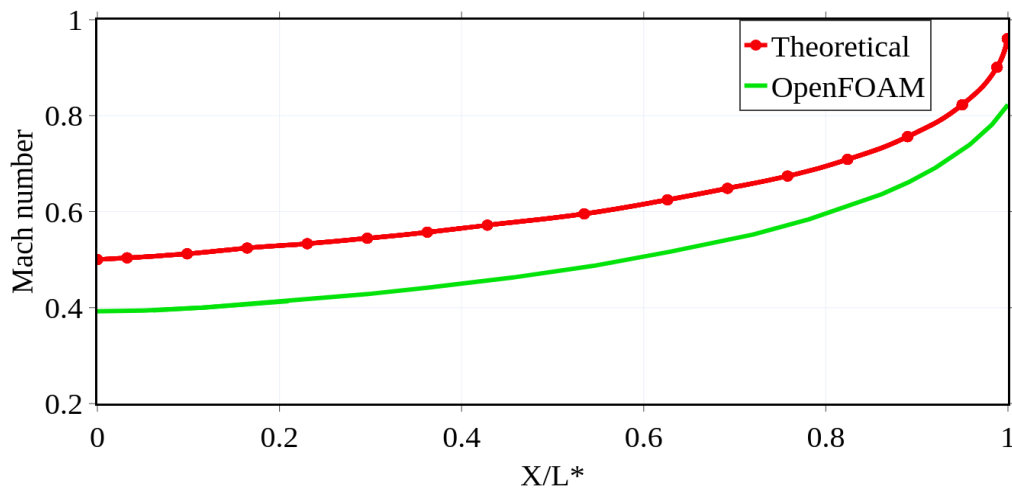
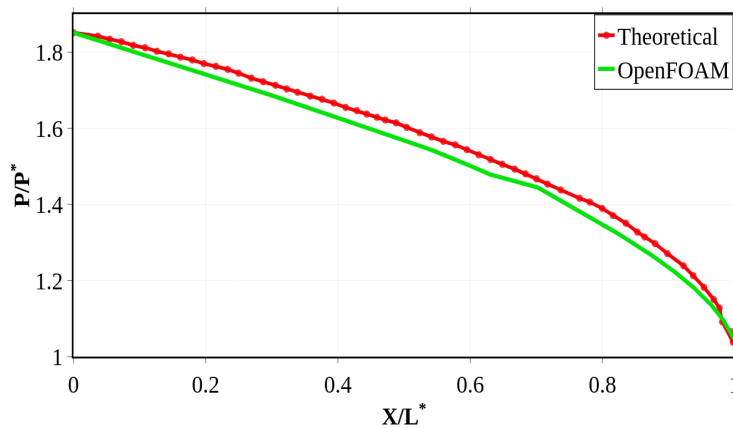


**Fig 8:** Mach number distribution for fanno flow

- The slight difference of the Mach no. at the inlet is because, in OpenFOAM the mass flow rate is not prescribed, rather the pressure boundary condition is specified.
- Pressure and Temperature plots show a very good agreement between analytical and numerical results.

## Case 1.2 Rayleigh Flow

Rayleigh Flow: Pressure Distribution



Rayleigh Flow: Temperature Plot

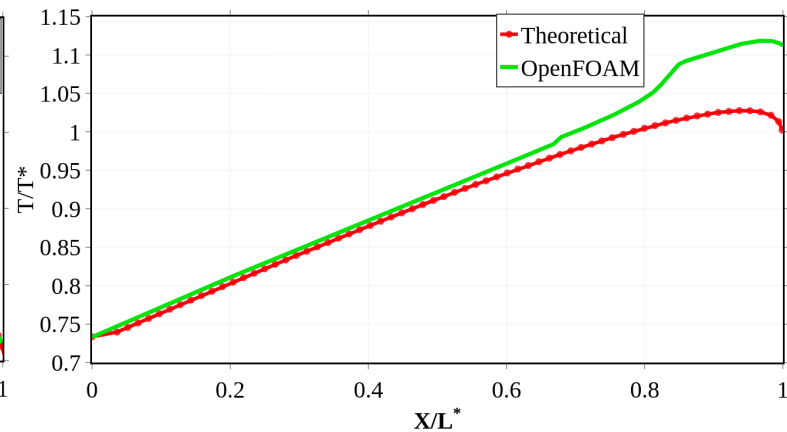


Fig 9: Pressure distribution for Rayleigh flow    Fig 10: Temperature distribution

Rayleigh Flow: Mach No. Plot

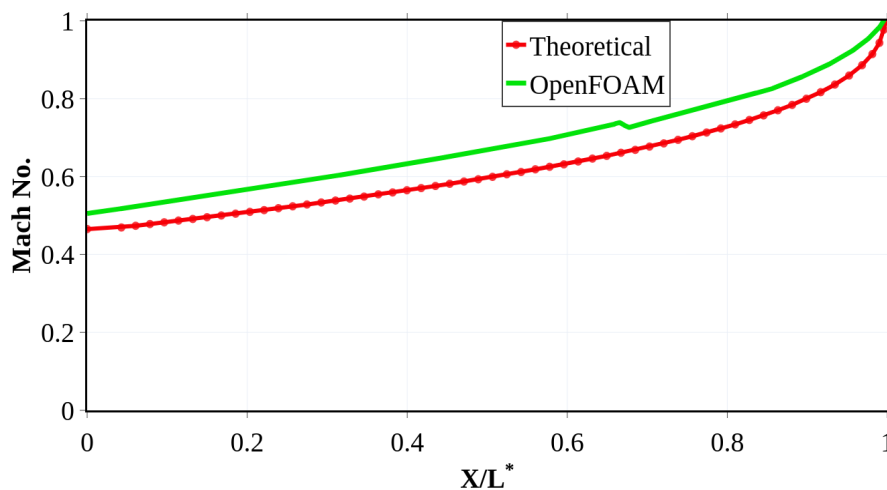


Fig 11: Mach number distribution

- For the Mach no. & pressure plots show a very good agreement between analytical and numerical results.
- A slight difference in the Temp. plots because of the method of application of heat i.e. the implementation of the heat flux boundary condition in OpenFOAM. Moreover we have utilised the symmetry of the geometry and have used a wedge whereas in the paper, there was no mention about the shape of the mesh. Also they used a one-dimensional model whereas we have used a two-dimensional model. Hence, a comparative trend of the plot is sought and it is seen that both the curves follow the same trend.

### Case 1.3 Combined Friction and Heat Transfer

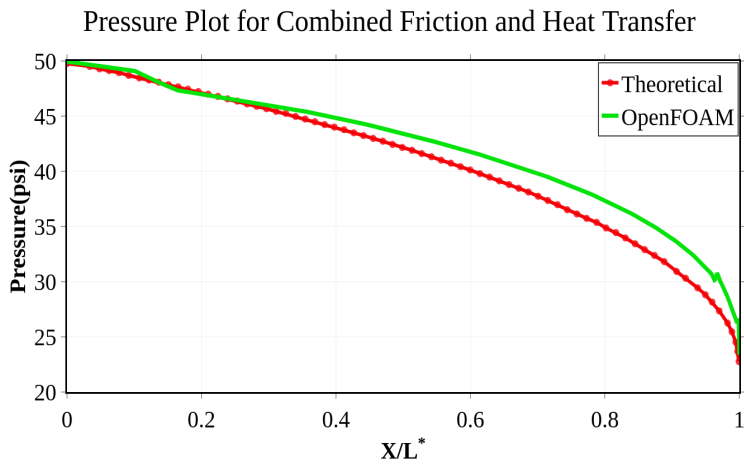


Fig 12: Pressure distribution

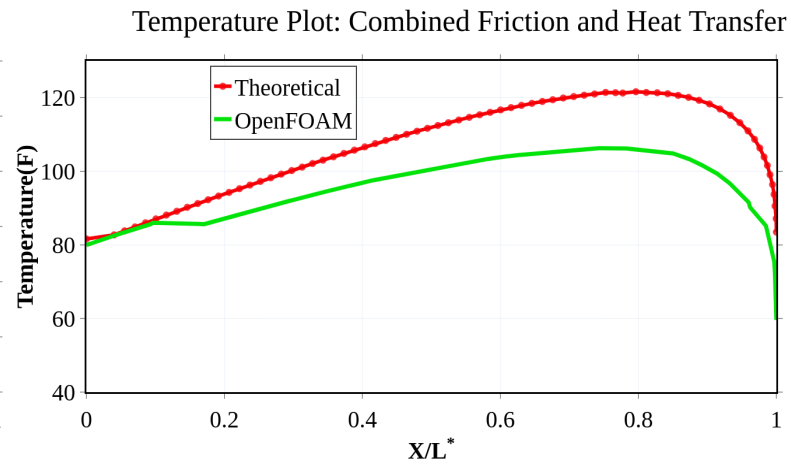


Fig 13: Temperature distribution

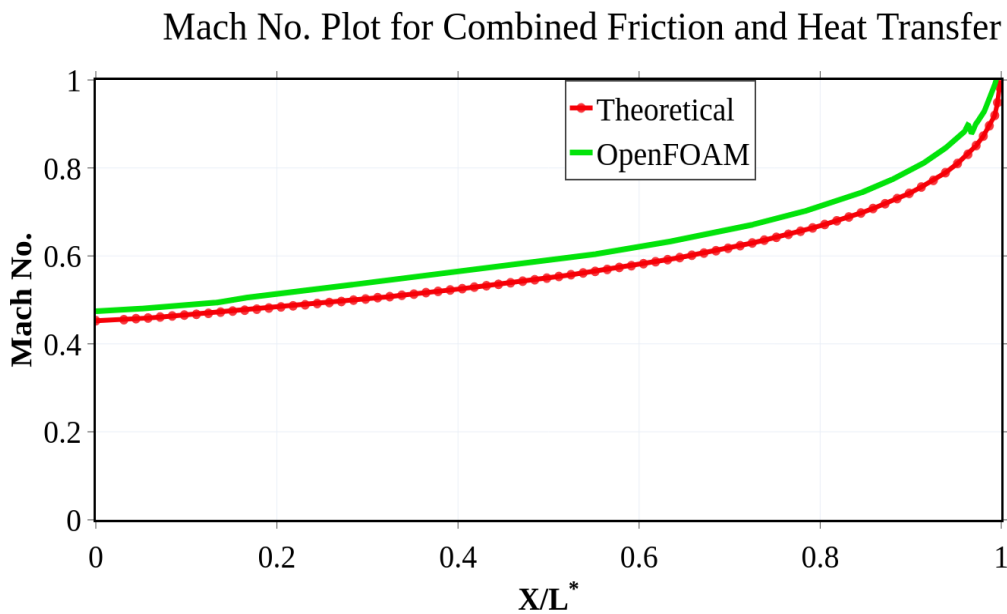
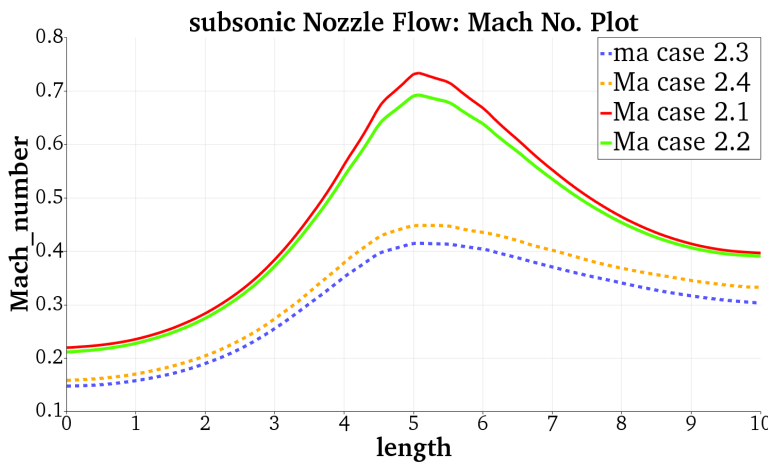


Fig 14: Mach number distribution

- For the Mach no. & pressure plots show a very good agreement between analytical and numerical results for this case also.
- Here also a slight difference in the Temp. plot is observed. The reason for this is explained as above in the Rayleigh flow section.

**Subsonic (compare the trends of the graph)**



**Fig 15** Mach number distribution for **case 2**

- The trends of the graph for the case 2.3 & 2.4 have quite a match with the reference case graph [1].
- And for the case 2.1 & 2.2, by adding the heat flux, Temp. also increases and for the gases, viscosity increases with increasing temperature. And hence the Mach no. decreases.

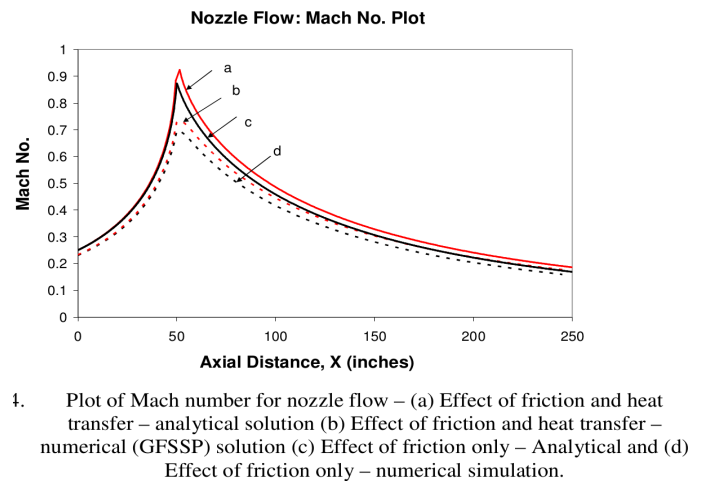


**Fig 16** Mach number distribution for the reference case [1]

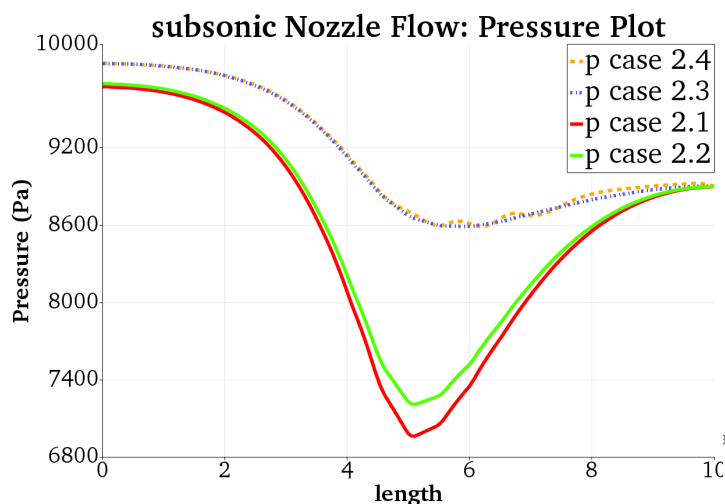


**Fig 17** Pressure distribution for **case 2**

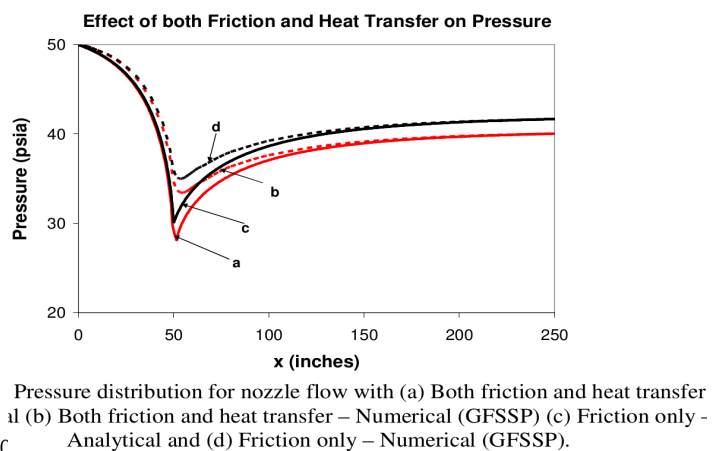


**Fig 18** Pressure number distribution for the reference case [1]

- The graphs for our cases (2.3 and 2.4 of fig. 17) are more or less coincident whereas in the paper (cases b and d of fig. 18), it shows a slight difference mainly at the diverging part of the nozzle. This is because the outlet pressure boundary condition was not given explicitly in the paper and we have kept a fixed value boundary condition for outlet pressure in both our cases.

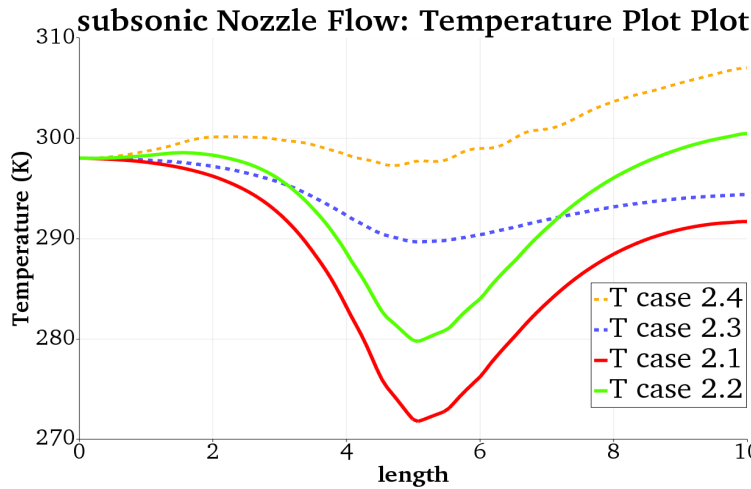
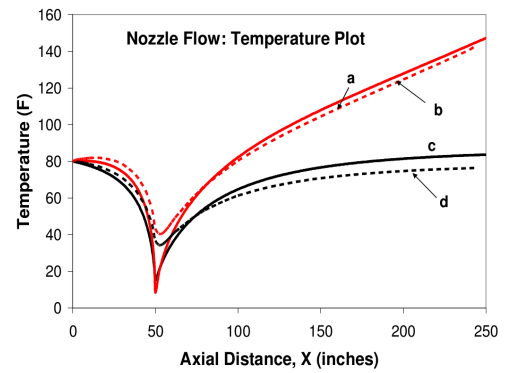


Fig 19 Temperature distribution for case 2



Temperature distribution for nozzle flow with (a) Both friction and heat transfer - Analytical (b) Both friction and heat transfer - Numerical (GFSSP) (c) Friction only - Analytical and (d) Friction only - Numerical (GFSSP).

Fig 20 Temperature number distribution for the reference case [1]

- Here the trends of the graphs for temperature are similar for our case (cases 2.3 and 2.4 of fig. 19) and the paper (cases b and d of fig. 20). The differences in values are due to the fact that the amount of heat flux was not given in paper and we used an arbitrary but suitable value of  $5000 \text{ W/m}^2$ .
- In fig. 19, case 2.1 is the normal case i.e. without considering friction or heat transfer and case 2.2 is the case which takes in account only heat transfer. In case 2.2, a heat flux of  $5000 \text{ W/m}^2$  is given to the nozzle and hence the temperature in every part of the nozzle is greater than that of case 2.1, which is obvious.

supersonic

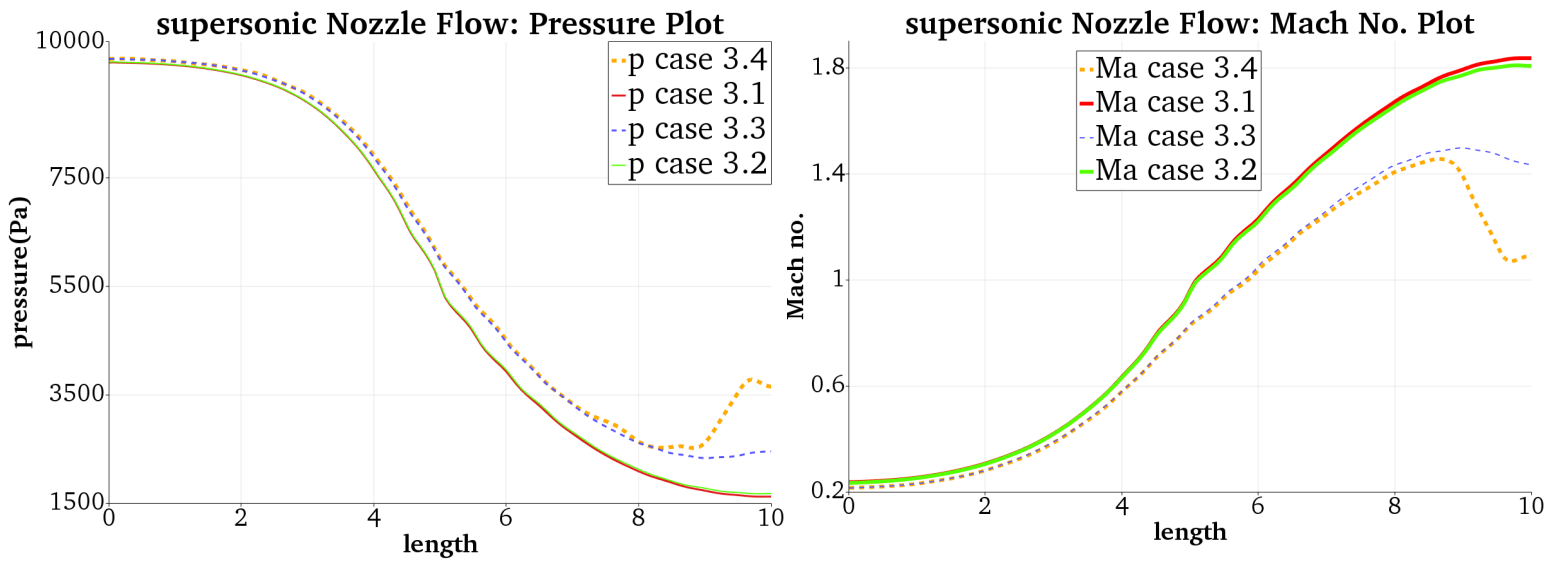


Fig 21 Pressure number distribution for case 3 Fig 22: Mach number distribution for case 3

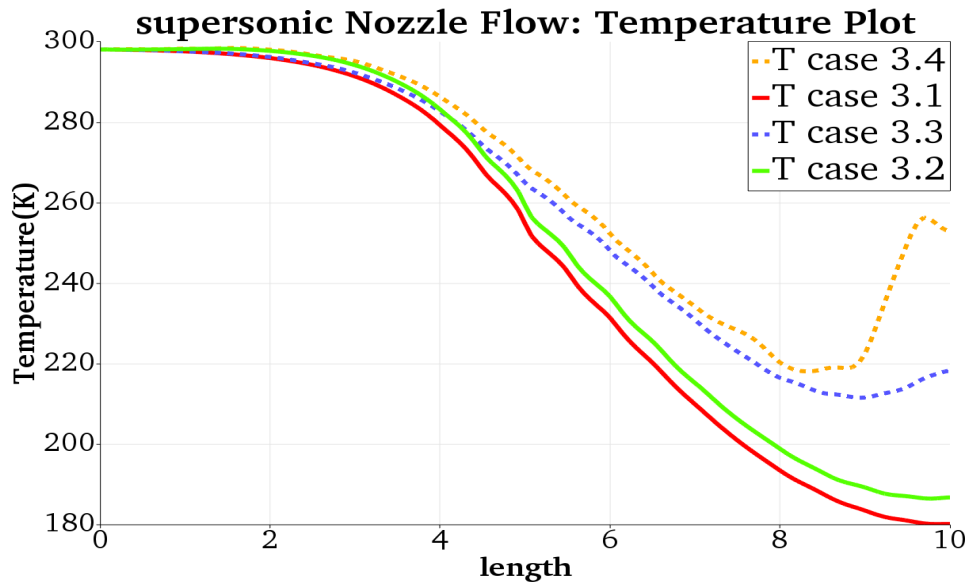


Fig 23: Temperature distribution for case 3

- In fig. 23, the temperature plot for the case 3.4 (involving both friction and heat transfer) is notable, mainly the sudden temperature rise near the outlet. Fig. 3.3 (involving only friction) also shows a similar trend but the rise is less. Both the cases are supersonic and in supersonic, temperature is constrained to decrease along the length, which indeed is the outcome for all the cases (3.1, 3.2, 3.3 and 3.4). For cases 3.1 and 3.2, the temperature keeps on decreasing. For the case 3.4, the temperature decreases due to the supersonic constraint. But heat is externally

added to case 3.4 and is also generated due to friction and this heat addition and/or generation manifests itself as a sudden rise in temperature near the outlet.

So, the conclusion is that even if we supply uniform heat flux throughout, temperature keeps on decreasing if the flow is supersonic (like case 3.2) and rises suddenly near the outlet for case 3.4, the reason for which is explained above.

Also it is seen that temperature is greater for the cases involving friction (like case 3.3) than the cases without friction (like case 3.1). This is mainly due to heat generation due to frictional dissipation.

- Mach no. is less for the cases involving friction than the cases without involving friction, which is intuitive as friction decreases the flow velocity.

### Supersonic with shock

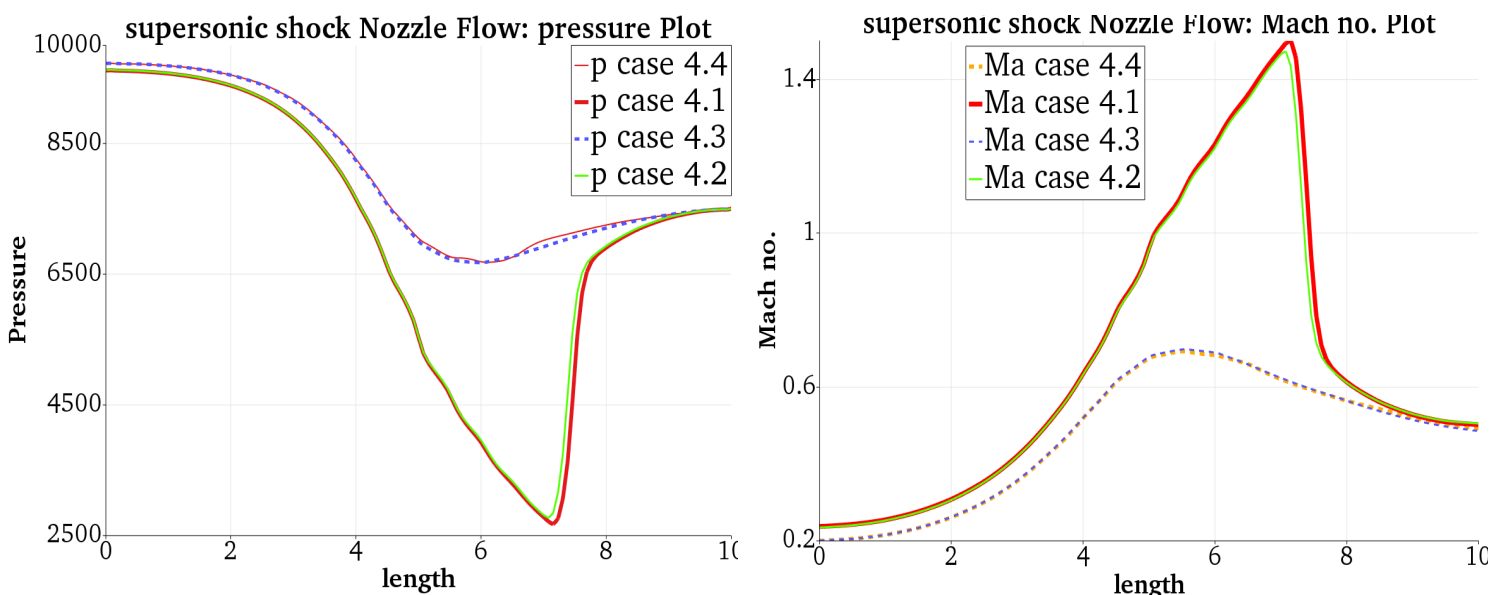


**Fig 24:** Pressure number distribution for **case 4** **Fig 25:** Mach number distribution for **case 4**

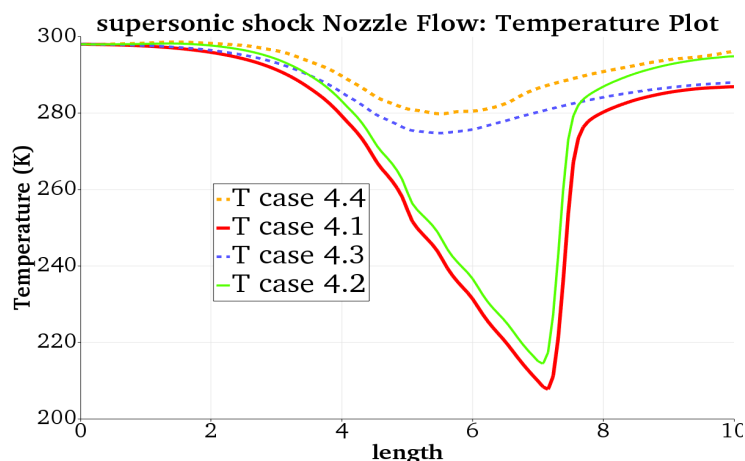


**Fig 26:** Temperature distribution for **case 4**

- In all the above cases, namely case 4.1, 4.2, 4.3 and 4.4, a fixed value boundary condition is applied at the outlet. We observe that for the above value of 7500 Pa at the outlet, the flow becomes supersonic for cases 4.1( normal case) and 4.2( case involving only heat transfer) and a shock is observed at some distance from outlet as the imposed outlet pressure is not the design pressure.  
However, for the remaining cases which involve friction such as case 4.3( only friction) and case 4.4( both friction and heat transfer), a supersonic flow could not be obtained for the above imposed value of 7500 Pa at outlet and the flow remains subsonic throughout the whole regime, which is also confirmed from the nature of their graphs.
- Another interesting thing to note is that, even by adding a substantial amount of heat, the shock position does not change significantly (observed by the shock positions of case 4.1 and 4.2)

## Conclusion:

This paper presents a numerical study of the effect of various parameters in deLaval nozzle like friction, heat transfer and area change in various regimes of compressible flow like subsonic, supersonic and supersonic with shock. In the design of deLaval nozzle friction and Heat-flux generated at the wall are one of the major factors usually missed out. The numerically obtained solutions of temperature, pressure and Mach number have been compared with the solution given in the paper for two different subsonic cases representing the effect of friction and heat transfer.

There is a good agreement between the results given in paper and the results obtained in the OpenFoam. We have extended our case to supersonic and supersonic with shock as well. Conclusions have been drawn based on the simulation predictions. Their adherence to observed data and/or theoretical predictions will have to be verified and will be the future scope of this work.

## Reference

- [1] Bandyopadhyay, Alak, and Alok Majumdar. "Modeling of Compressible Flow with Friction and Heat Transfer using the Generalized Fluid System Simulation Program (GFSSP)." Thermal Fluid Analysis Workshop. Vol. 10 (2007): Web. 20 January 2017.
- [2] <https://cf.fossee.in/case-study-project/case-study-run/69>
- [3] NPARC Alliance Verification and Validation Archive. Steady, Inviscid Flow in a Converging-Diverging Verification (CDV) Nozzle.
- [4] OpenFOAM User Guide, Version 7